



Quantifying surface fuels for fire modelling in temperate forests using airborne lidar and Sentinel-2: potential and limitations

Pia Labenski^{a,*}, Michael Ewald^a, Sebastian Schmidlein^a, Faith Ann Heinsch^b, Fabian Ewald Fasnacht^c

^a Institute of Geography and Geoecology, Karlsruhe Institute of Technology (KIT), Kaiserstr. 12, 76131 Karlsruhe, Germany

^b USDA Forest Service, Rocky Mountain Research Station, 5775 US Highway 10 West, Missoula, MT 59808, USA

^c Department of Remote Sensing and Geoinformation, Institute of Geographic Sciences, Freie Universität Berlin, Malteserstr. 74-100, 12249 Berlin, Germany

ARTICLE INFO

Edited by Marie Weiss

Keywords:

Surface fuels
Remote sensing
Fire behaviour
Temperate forests
Random forest regression

ABSTRACT

Surface fuel information is an essential input for models of fire behaviour and fire effects. However, spatially explicit, continuous information on surface fuel loads and fuelbed depth is scarce because the collection of field data is laborious, while suitable methods for deriving estimates from remote sensing data are still at an early stage of development. Fine-scale surface fuel mapping using both passive and active remote sensing has not yet been carried out in Central European forest types, and it remains unexplored how prediction uncertainties of different fuel components affect modelled fire behaviour. This study combines very detailed airborne lidar and multispectral satellite data to extract metrics describing forest structure and composition in two forested areas in southwestern Germany. These metrics were used to predict field-sampled surface fuel components using random forest regression. Accuracies of continuous fuel load predictions were compared to accuracies that could be achieved if only forest type-specific average fuels were assigned. Results revealed that models based on remotely sensed metrics explain part of the variance in litter and fine dead woody fuels ($R^2=0.27-0.41$), but not in coarser dead woody fuels. Estimates for herb and shrub fuels were fairly accurate ($R^2=0.55-0.64$) but limited for the more fire-relevant fine fraction of shrub fuels ($R^2=0.39$). Fuelbed depth was moderately well predicted based on remote sensing data ($R^2=0.44$). Lidar-derived metrics were particularly useful for predicting understory fuels and fuelbed depth. Litter and fine woody fuel predictions were linked to canopy characteristics captured with both lidar and multispectral data and similarly accurate estimates could be obtained using average values based on forest type. We used the fine-scale surface fuel maps derived from remote sensing to predict potential surface fire behaviour in the study area and analysed the sensitivity of modelled fire behaviour to errors in the predicted loads of different surface fuel components: fire behaviour was most sensitive to errors in litter and especially shrub fuel loads, hence estimates of these components need to be improved. Overall, this study showed that statistical relationships between remotely sensed metrics describing forest composition and structure and surface fuels have some potential for estimating fuel loads in Central European forest types and should be further developed to provide starting points for realistic fire behaviour models.

1. Introduction

Fire risk in temperate forests of Central Europe has long been of minor concern to many countries. However, recently the danger of catastrophic fire events in these formerly low-risk areas has risen as result of climate change (de Rigo et al., 2017). The year 2022 has shown that the trend of increased wildfire activity associated with prolonged droughts in Central Europe continues, with the number of fires and areas

burned exceeding long-term averages (EFFIS, 2023a). Weather conditions favouring wildfire ignition and spread are projected to become more frequent (IPCC, 2021), making the occurrence of catastrophic fires worldwide 1.31 to 1.57 times more likely by the end of the century (UNEP, 2022). While fires are an integral part of the natural disturbance regime in some ecosystems (Battisti et al., 2016), uncontrolled wildfires can have serious social, economic and environmental impacts, such as loss of wildlife habitats, disease from toxic smoke, destruction of

* Corresponding author.

E-mail address: pia.labenski@kit.edu (P. Labenski).

<https://doi.org/10.1016/j.rse.2023.113711>

Received 24 March 2023; Received in revised form 7 June 2023; Accepted 3 July 2023

Available online 17 July 2023

0034-4257/© 2023 Elsevier Inc. All rights reserved.

infrastructure and property, and feedbacks to climate change through greenhouse gas emissions (UNEP, 2022). To mitigate adverse effects of wildfires under global warming, it is important to better understand fire behaviour especially in ecosystems where this has not been studied extensively. The latter include temperate forests of Central Europe. One important aspect to investigate is how fire behaviour and fire effects are related to forest stand properties such as the amount and distribution of combustible organic material, i.e. fuel.

Spatially explicit fuel information is used for simulations of fire spread, intensity and severity (Finney, 2006; Tymstra et al., 2010), planning of management activities such as fuel reduction treatments (Moghaddas et al., 2010; Furlaud et al., 2018) and strategic planning of fire suppression efforts (Page et al., 2013; Plucinski, 2019). It is also needed to estimate emissions of greenhouse gases and particulate matter from burned areas (Ottmar, 2014; Weise and Wright, 2014). Several concepts have been developed to describe fuels and their characteristics, often with focus on specific applications like fire behaviour prediction (Burgan and Rothermel, 1984; Cruz and Fernandes, 2008) or fire effects and emission modelling (Reinhardt, 1997; Prichard et al., 2007). However, one fuel variable that is used in almost all fire management applications is fuel load, i.e. biomass per unit area (Keane, 2013). Fuel load is commonly specified for each fuel component of a fuelbed: surface fuelbeds (< 2 m) are composed of litter, shrubs and herbs as well as down woody material stratified into different particle diameter classes based on their rate of drying (Fosberg et al., 1970). Surface fuel loads vary at very fine spatial scales (metres to submetres) (Keane, 2015) and drive local fire behaviour: The heterogeneous distribution of dense woody fuels has for example been linked to variations in fire intensity (Loudermilk et al., 2012), which has implications for tree mortality, post-fire plant diversity and other long-term ecosystem effects (Mitchell et al., 2009; Dell et al., 2017). Understorey vegetation such as grasses, forbs and shrubs form loosely packed fuelbeds and thus have a strong influence on fire dynamics (Keane, 2015), which can be important to consider when developing effective firefighting tactics. An important variable in this context is fuelbed depth (average height of the surface fuels), which together with fuel load determines the bulk density of the fuelbed. In forest stands without understorey and without coarse deadwood, the fuelbed depth is equal to the litter depth. Litter provides a continuous, easily ignitable fuel source in almost all forest stands, capable of supporting the contagious spread of surface fires. As most fires burn through surface fuels (Albini, 1984), fine-scale maps of surface fuel loads and fuelbed depth are useful for assessing spatial patterns in fire behaviour characteristics and fire effects. High-resolution surface fuel maps are particularly important when fires are generally small in size and crown fires do not play a major role, as is the case for most forest fires in Central Europe (San-Miguel-Ayanz et al., 2021).

Remote sensing approaches offer the potential to efficiently create and update continuous fuel maps across large areas. However, as pointed out by Gale et al. (2021), the focus in current fuel remote sensing literature is on estimating overstorey fuel variables (Riaño, 2003; Andersen et al., 2005; García et al., 2012; González-Ferreiro et al., 2017; Botequim et al., 2019), while studies on surface fuel variables are underrepresented. This may be due to the difficulty of estimating fuel properties beneath canopies using airborne or spaceborne sensors. Gale et al. (2021) also noticed a tendency towards discrete mapping of surface fuels as fuel types or fuel models instead of mapping continuous fuel variables (Seielstad and Queen, 2003; Mutlu et al., 2008; García et al., 2011; Chirici et al., 2013; Marino et al., 2016; Domingo et al., 2020). Such classifications into fuel types or fuel models summarise the fuel information needed for specific modelling purposes in broad categories (Lutes et al., 2009), which are usually assigned to an entire stand, disregarding the more complex and fine-scale distribution of fuels in the forest (Loudermilk et al., 2022). Categorising fuel information, e.g. by averaging field-measured loads and associating them with a forest type, may be useful for rapid fuel assessments, but fuel loads and fuelbed depth are inherently continuous variables (Keane, 2015). Accurate

quantification of continuous variables is challenging due to the high spatial and temporal variability of surface fuels, which can also differ for the individual fuel components (Keane, 2015). Studies predicting different components of surface fuels using passive and active remote sensing technologies report strongly varying model performances depending on study area, sensor used and scale of the investigation as well as the inclusion of auxiliary variables (Table 1). Hence, the utility of remote sensing for fine-scale mapping of surface fuel loads in previously unexplored ecosystems remains an open question. A comparison between the accuracy of continuous fuel estimates and average values associated with forest types may be helpful in future decisions on how to efficiently map fuel components in these forest types. In addition, there are no studies that have investigated the extent to which errors in remotely sensed surface fuel estimates affect fire models based on them.

Multispectral remote sensing data have been used to classify vegetation types and extract stand characteristics, which are then used to estimate surface fuel loads with empirically derived relationships (Brandis and Jacobson, 2003; Jin and Chen, 2012). However, surface fuel loads are not always correlated with forest stand attributes (Keane et al., 2012) and can vary considerably within a vegetation type (Keane, 2015). Other studies have integrated multispectral information with other remotely sensed biophysical variables and fire history data to explain surface fuel load variation (Reich et al., 2004; Duff et al., 2013; Peterson et al., 2013). Topography, climate variables and time since last fire were found to be important predictors of fuel load variation in these study areas encompassing rather complex terrain with multiple vegetation types and/or frequent fire disturbance. Comparatively little variation in surface fuel load could be explained by spectral information and vegetation indices alone at more homogeneous sites (Arellano-Pérez et al., 2018), while satellite-derived fractions of vegetation cover were useful to explain surface fuel load variation across diverse Cerrado vegetation types (Franke et al., 2018). These results indicate that multispectral remote sensing data from passive sensors such as Landsat and Sentinel-2 can explain a certain fraction of surface fuel load variability, as they carry information related to vegetation density and species composition, which are likely to drive understorey presence and the type and amount of litter. However, fine-scale variation of surface fuel components is not adequately captured with these data; hence active remote sensing systems like airborne lidar (ALS), which are able to partly penetrate canopies and collect information about vertical forest structure and the forest floor, may be useful in the direct mapping of laying trunks, shrubs or even the presence of herbs and grasses. Accordingly, ALS has been used in several studies to estimate components of surface fuels based on statistical relationships with height, density and intensity metrics of the reflected laser pulses (Skowronski et al., 2007; Jakubowski et al., 2013; Hudak et al., 2016); however, so far with only moderate reliability for predictions of ground-based fuels. One reason for this might have been limited point densities which lead to comparably sparse information on understorey vegetation and forest floor roughness, particularly if rather dense overstorey vegetation is present, which is the case in most Central European forests. As an alternative, terrestrial laser scanning (TLS) and photogrammetric approaches allow to collect dense point clouds for more accurate surface fuel estimations (Chen et al., 2017; Wallace et al., 2017; Li et al., 2021). However, these techniques are less suitable for mapping fuels across large areas, although they provide detailed information about below-canopy structure that can support models based on ALS data (Alonso-Rego et al., 2021). Fusion of ALS with multispectral data can provide both direct and indirect measurements of surface fuels and may thus lead to more accurate mapping both within and across different forest types. Studies combining ALS with multispectral information have found moderate improvements in predicting surface fuel load variation in coniferous forests (Bright et al., 2017; Stefanidou et al., 2020). However, it remains unclear whether a combination of multispectral satellite and airborne lidar data is suitable to map surface fuel load and fuelbed depth variation in temperate mixed broadleaf and conifer forests

Table 1
Overview of studies estimating surface fuel loads with remote sensing data.

| | sensor (spatial resolution) | fuel component | study area | explained variance | method | independent variables |
|------------------------------|--|--|---|--------------------|---|--|
| Brandis and Jacobson (2003) | Landsat TM (30 m) | litter and fine fuel load | eucalypt forest, woodland, shrubland, Australia | - | classification techniques | vegetation type, vegetation indices, fire history data, biomass turnover rates |
| Jin and Chen (2012) | Landsat, (30 m), QuickBird (2m) | litter, 1 hr, 10 hr, 100 hr, 1000 hr loads | larch-dominated boreal forest, China | 5-57 % | linear regression | spectral bands, stand-characteristics |
| Reich et al. (2004) | Landsat TM (30 m) | litter, duff, 1 hr, 10 hr, 100 hr, 1000 hr | Black Hills National Forest, South Dakota | 34-45 % 55-72 % | multiple regression analysis, binary regression trees | spectral bands, topography, forest class |
| Duff et al. (2013) | Landsat 5, remotely sensed biophysical data (50 m) | litter, elevated fuels (shrubs, herbs), bark fuel | eucalyptus woodland, Australia | 30-51% | generalized additive models | NDVI, topography, climate, soil properties, fire history |
| Peterson et al. (2013) | Landsat TM | 1 hr live fuels, 1 hr, 10 hr, 100 hr fuels; discretized into three classes | chaparral shrublands to subalpine forests, Yosemite National Park, California | - | random forest | spectral bands, vegetation indices, topography, climate, soil properties, fire history |
| Arellano-Pérez et al. (2018) | Sentinel-2 (10-20m) | total surface fuel load | even-aged pine stands, North western Spain | 12 % | random forest, multivariate adaptive regression splines | spectral bands and vegetation indices |
| Franke et al. (2018) | Landsat 8, Sentinel-2 | total surface fine fuel load | Cerrado, Brazil | 86 % | mixture tuned matched filtering | non-photosynthetic dry vegetation and soil fractions per pixel |
| Skowronski et al. (2007) | ALS (pulse spacing 0.125 m) | presence of ladder fuels | Pinelands, New Jersey | - | - | vertical height bins of lidar returns |
| Jakubowski et al. (2013) | ALS (9 pts/m ²), multispectral imagery (1 m) | total surface fuel load, 1000 hr load, understory shrub cover and height | mixed-conifer forest, Nevada | 32-48 % 59-62 % | support vector machines, linear and additive regression | spectral values, topography, lidar metrics |
| Hudak et al. (2016) | ALS (6.9 pts/m ²) | total surface fuel load | longleaf pine forest, Florida | 32-44 % | multiple linear regression | lidar metrics |
| Wallace et al. (2017) | TLS (0.018 ° between points), image derived point-clouds | surface vegetation biomass up to 25 cm | eucalypt forest, Australia | 74 % | linear regression | TLS derived and point-cloud derived vegetation volume |
| Li et al. (2021) | TLS (> 1 pt/cm ³) | herb and shrub layer biomass | temperate forests, northeastern China | 69-72 % | linear and nonlinear regression | TLS-derived understory height, cover and vegetation volume |
| Chen et al. (2017) | TLS, ALS (footprint: 0.26 m) | total surface fuel load | eucalypt forest, Australia | 89 % | multiple regression analysis | terrain features, forest structural characteristics, fire disturbance, fuel and burn types |
| Alonso-Rego et al. (2021) | ALS (0.5 pts/m ²), TLS (130 pts/m ²) | litter and duff, understory load, down woody debris load | even-aged pine stands, NW Spain | 35-49 % | multivariate adaptive regression splines | TLS and ALS metrics |
| Bright et al. (2017) | ALS (2 pts/m ²), Landsat time series (30 m) | litter, duff, 1 hr, 10 hr, 100 hr, 1000 hr loads | coniferous montane forest, Colorado | 24-32 % | random forest | lidar height and density metrics, LandTrendr variables, topography |
| Stefanidou et al. (2020) | multispectral ALS, (83 pts/m ²) | litter, grass and forbs, 1 hr, 10 hr, total surface fuel load | Abies borisii, hybrid fir, dense coniferous forest, Greece | 59-71 % | multiple linear regression analysis | lidar height and intensity metrics |

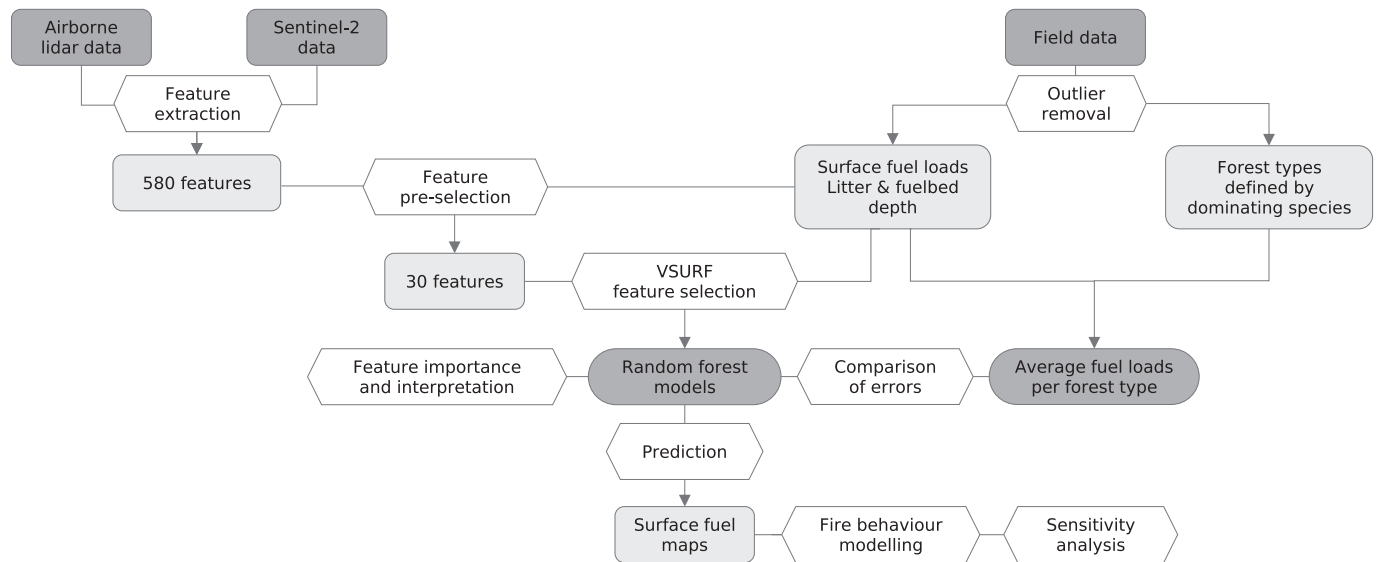


Fig. 1. Overview of the data used and analyses carried out in this study.

characterised by high structural heterogeneity at fine spatial scales. The focus of this study is on mixed stands of deciduous beech and oak as well as pine and Douglas fir in lowland to colline regions. The relationship between overstorey composition and surface fuel loads needs to be better understood for these forests in order to assess whether simplistic associations of surface fuel loads with broader vegetation categories such as forest types are justified to predict variability in potential fire behaviour and can be used as an alternative to fine-scaled remote sensing maps. At last, given the frequently reported inaccuracies in surface fuel estimation, it is critical to understand the sensitivity of current fire behaviour models to such inaccuracies. Therefore, the aim of this work is to

- i) explore the ability to predict surface fuel loads and fuelbed depth in heterogeneous mixed forests of Central Europe using freely available high-resolution Sentinel-2 data (10-20 m) combined with high-density ALS data (> 72 points/m²)
- ii) improve our understanding of remote sensing-based predictions of surface fuels by analysing a large set of features as proxies for vegetation structure and composition across vertical forest strata and investigate whether average fuel loads based on forest types can be used in practice
- iii) assess the influence of errors in surface fuel load estimates on modelled fire behaviour by performing a sensitivity analysis.

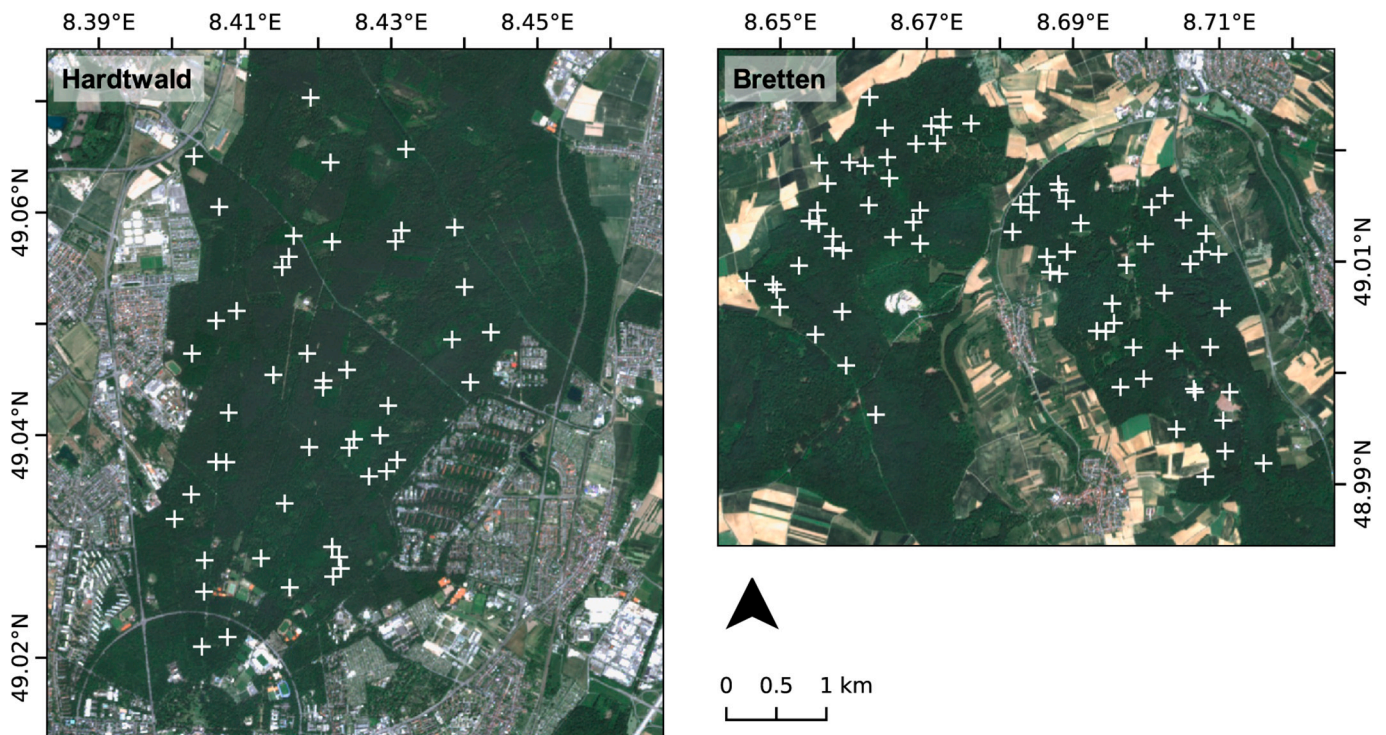


Fig. 2. Overview of the two study areas ‘Hardtwald’ (left) and ‘Bretten’ (right). White crosses indicate the center locations of the field plots. Background image is a Sentinel-2 scene from May 2020 obtained from USGS Earth Explorer (U.S. Geological Survey, 2023).

Table 2

Area share of the four main forest types in each study area, as well as the area share of different age classes within each forest type. Data extracted from ForstBW (2019) and ForstBW (2023).

| forest type | study area | % study area occupied | % forest type area occupied | | | |
|-------------|------------|-----------------------|-----------------------------|-----------|------------|----------|
| | | | age <40 | age 40-80 | age 80-120 | age >120 |
| pine | Hardtwald | 69 | 7 | 32 | 26 | 35 |
| | Bretten | 13 | 0 | 34 | 66 | 0 |
| beech | Hardtwald | 9 | 6 | 56 | 35 | 3 |
| | Bretten | 44 | 7 | 23 | 39 | 31 |
| oak | Hardtwald | 12 | 5 | 95 | 0 | 0 |
| | Bretten | 9 | 18 | 28 | 46 | 8 |
| Douglas fir | Hardtwald | 3 | 3 | 86 | 10 | 0 |
| | Bretten | 27 | 12 | 48 | 40 | 0 |

2. Methods

2.1. Overview

The main steps of the analysis are summarised in Fig. 1. First, we preprocessed the field measurements of surface fuel loads as well as litter and fuelbed depth in our study area (sections 2.2 and 2.3). We obtained average surface fuel loads for the main four forest types of our study area. We then processed the high density lidar and multispectral datasets by using a combination of different techniques and obtained a large number of potential predictors of surface fuels (sections 2.4 and 2.5). After feature selection (section 2.6), we trained random forest models to predict surface fuel loads based on the selected remotely sensed predictors (section 2.7) and compared the errors of the method with the errors of using average surface fuel loads per forest type (section 2.8). Furthermore, we investigated the importance of different predictors to better understand the relationship between surface fuels and forest composition and structure (section 2.9). Then, we predicted surface fuel maps for our study area (section 2.10) and modelled the potential fire behaviour (section 2.11). Finally, we performed a sensitivity analysis to assess the influence of the predicted fuel components on modelled fire behaviour (section 2.12).

2.2. Study area

Field data were collected in two study areas of temperate mixed forest in south-western Germany. The *Hardtwald* forest (19.6 km²) is located in the flat upper Rhine valley (49.037 N, 8.416 E) at 120 m a.s.l., and the *Bretten* municipal forest (10.5 km²) in the Kraichgau hills (49.006 N, 8.699 E) at 180 to 300 m a.s.l. (Fig. 2). The two study areas are characterised by temperate climate with mean annual temperatures of 11.4 °C (*Hardtwald*) and 10.2 °C (*Bretten*) in the reference period from 1991 – 2020 (DWD Climate Data Center, 2023), with monthly mean temperatures varying between 1.1 and 21.5 °C at the *Hardtwald* site, and between 0.2 and 19.8 °C in *Bretten*. Mean annual precipitation amounts to 746 mm in *Hardtwald* and 792 mm in *Bretten*.

The examined forest stands are diverse in age and structure (Table 2), encompassing dense, young planted stands of Scots pine (*Pinus sylvestris* L.) as well as older, pine-dominated stands with an understory of black cherry (*Prunus serotina* Ehrh.) or European beech (*Fagus sylvatica* L.). They further include mature beech stands with closed canopies and

areas dominated by natural regeneration of beech. There are old, open stands of sessile oak (*Quercus petraea* Liebl.), as well as row-wise plantations of sessile oak and red oak (*Quercus rubra* L.), and finally young and mature stands of Douglas fir (*Pseudotsuga menziesii* (Mirb.) Franco), the latter either pure or mixed with beech. Other, less frequently occurring species include hornbeam (*Carpinus betulus* L.), European larch (*Larix decidua* Mill.), Norway spruce (*Picea abies* (L.) H. Karst), pendunculate oak (*Quercus robur* L.), silver fir (*Abies Alba* Mill.) and poplar (*Populus* spp.). The area share of the main forest types is 69 % pine, 12 % oak, 7 % beech, 3 % Douglas fir and 9 % other in the *Hardtwald* (ForstBW, 2023), and 44 % beech, 27 % Douglas fir, 13 % pine, 9 % oak and 7 % other in the *Bretten* forest. (ForstBW, 2019).

Although precipitation in the region is generally evenly distributed throughout the year, an increase in heat days and prolonged droughts during the summer months has been observed in recent years (DWD Climate Data Center, 2023), leading to increased drought stress and damage to various tree species, especially on the sandy soils of the Rhine valley. So far, there have been no major forest fires in the study area (and no recordings by EFFIS (2023b) between 2018 and 2023), but in the hot and dry August of 2022 there were several smaller fires (0.1 to 5 ha) in the *Hardtwald*, presumably caused by arson (ka-news, 2022). Given the expected increase in fire risk in the future, an understanding of the fuel situation in these forests and its relationship to fire behaviour is needed to better prepare for managing such fires.

2.3. Field data

Surface fuels were inventoried from May to September 2020 and 2021 in 119 circular field plots (radius = 7.5 m, area = 176.6 m²) distributed in a stratified random sampling across the study areas. Information on dominating canopy tree species, as available from stand maps based on forest inventories that are part of the German Forsteinrichtung (ForstBW, 2019, 2023), was used for stratification. The measured surface fuel components in each field plot include all dead and live fuels within 2 m above the ground: litter, dead woody fuels separated into 1 hr, 10 hr, 100 hr and 1000 hr fuels, live herbaceous fuels (hereafter referred to as herb fuels), mosses, and live woody fuels (young trees and shrubs, hereafter referred to as shrub fuels). Fuel loads were obtained for all surface fuel components following the protocol by Woodall and Monleon (2008). As most operational fire behaviour models are based on the Rothermel equation (Rothermel, 1972), which

Table 3

Overview of the number of field plots in different forest types and per class of mean DBH and tree count.

| | all | DBH ≤ 20 cm (tree count > 15) | 20 cm < DBH ≤ 40 cm (5 < tree count ≤ 15) | DBH > 40 cm (tree count ≤ 5) |
|-------------|-----|----------------------------------|--|---------------------------------|
| beech | 25 | 5 (11) | 14 (11) | 6 (3) |
| oak | 25 | 10 (7) | 11 (14) | 4 (4) |
| pine | 29 | 6 (7) | 19 (13) | 4 (9) |
| Douglas fir | 29 | 3 (15) | 8 (10) | 18 (4) |
| other | 11 | 0 (5) | 7 (6) | 4 (0) |

Table 4
Overview of the predictors calculated from airborne lidar and Sentinel-2 data.

| source | predictor type | features | aggregation on plot-level | stand layer | vertical strata (lower height - upper height in m) | no. of features |
|---------------------|----------------|---|---|--|--|-----------------|
| Lidar | geometry | anisotropy, eigenentropy, omnivariance, sum of eigenvalues, linearity, planarity, sphericity, verticality, surface variation for neighborhood radii 0.5 and 1 m (equations in Table S2 in Supplementary Material) | mean | herb | 0.1-0.5, 0.25-0.5, 0.5-1 | 54 |
| | | | | shrub | 1-2, 2-3, 3-4, 4-5, 0.5-2, 0.5-5 | 108 |
| | | | | canopy | 5-10, 10-15, 15-20, 20-25, 25-30, 30-max, (max-1)-max, (max-2)-max, (max-5)-max | 162 |
| | density | no. points in each stratum relative to no. points within and below the stratum, no. points in each stratum relative to no. points in vertical column | - | herb | 0.1-0.5, 0.25-0.5, 0.5-1 | 6 |
| | | | | shrub | 1-2, 2-3, 3-4, 4-5, 0.5-2, 0.5-5 | 12 |
| | | | | canopy | 5-10, 10-15, 15-20, 20-25, 25-30, 30-max, (max-1)-max, (max-2)-max, (max-5)-max, 5-max, mean-max | 16 |
| | intensity | return intensity | mean, variation, standard deviation, coefficient of variation, skewness | herb | 0-0.5 | 5 |
| | | | | shrub | 0.5-2, 0.5-5 | 10 |
| | | | | canopy | (max-1)-max, (max-2)-max, (max-5)-max | 15 |
| | voxel | no. non-empty voxels per stratum, mean no. points per voxel per stratum, standard deviation of no. points per voxel per stratum, coefficient of variation of no. points per voxel per stratum, coefficient of variation of leaf area density per voxel per stratum, standard deviation of leaf area density per voxel per stratum | mean | herb | 0-0.5, 0.5-1 | 12 |
| shrub | | | | 1-2, 2-3, 3-4, 4-5 | 24 | |
| canopy | | | | 5-10, 10-15, 15-20, 20-25, 25-30, 30-max | 36 | |
| height | return height | maximum, quantiles (q99, q95, q90, q75, q50, q25, q10), mean, variance, standard deviation, coefficient of variation, skewness, kurtosis | all layers | - | 15 | |
| | | | herb | 0.1-0.5, 0.25-0.5 | 2 | |
| Sentinel-2 5 scenes | bands | B2, B3, B4, B5, B6, B7, B8, B8A, B11, B12 reflectances | area-weighted mean of plot-overlapping pixels | all/canopy | - | 50 |
| | indices | LAI, FCOVER, FAPAR, NDVI, EVI, NDMI, NDMI_2, SAVI, TCW, TCG | area-weighted mean of plot-overlapping pixels | all/canopy | - | 50 |
| total | | | | | | 580 |

assumes that only the fine biomass of the shrubs (plant parts < 6 mm in diameter, i.e. foliage and fine twigs) within 2 m above the forest floor contributes to surface fire spread, we calculated both total shrub woody biomass and shrub fine biomass within this 2 m height-layer to describe the shrub fuels. Details of the field measurements and data preparation are given in the Supplementary Material (S1). In addition to the fuel loads, we measured litter depth and the height of herbaceous and shrub layers and calculated the depth of the fuelbed by weighting the different fuel heights based on their contribution to total surface fuel load (Burgan and Rothermel, 1984). Species and diameter at breast height (DBH) of all trees in the plots were recorded, and the dominant overstory tree species in each plot was determined from the basal areas of the occurring tree species. This information was used to define the forest type (Table 3).

The field dataset was checked for outliers in the individual fuel components. In four fuel components, we removed 1-2 plots with loads far above the remaining data (> 5 times the standard deviation away from the mean of the data), which were not representative for the study area.

2.4. Lidar data

Lidar data of the study area were acquired in July 2019 using a Riegl LMS-VQ780i scanner on board a Cessna C207 aircraft. The flight was operated at an altitude of 650 m with a flight line overlap of 76 %. The lidar system acquired data at a pulse repetition rate of 1000 kHz with a scanning angle of $\pm 30^\circ$ from nadir. The signal was recorded as full waveforms with a footprint diameter of 0.16 m and then transformed into discrete points with an average spacing of 0.28 m, resulting in a point density of > 16 points/m² in a single flight line and a point density of > 72 points/m² with overlap in the final dataset. There was a time lag between the lidar acquisition (2019) and the field measurements (2020 and 2021), but no major disturbances (fire, windthrow or disease) occurred in the study area in the meantime.

A digital terrain model (DTM) at 0.5 m spatial resolution was calculated from the lidar point cloud using a surface estimation method based on active contours that matches an elastic surface to the assumed terrain points (lowest point in each cell of a raster area) by minimising an energy function (Elmqvist et al., 2001). The DTM was then subtracted from the raw point cloud to obtain a normalised point cloud. DTM calculation and subtraction were performed in TreesVis (Weinacker et al., 2004). From the normalised point cloud, all points falling into a field plot were extracted using FUSION (McGaughey, 2022). For each plot, a large number of metrics were calculated to comprehensively describe the arrangement of reflected pulses across vertical forest stand layers (herb layer from 0 to 0.5 m, shrub layer from 0.5 to 5 m and canopy from 5 m to top) and thus characterise vegetation structure at the plot-level (Table 4). In each stand layer, metrics computation was carried out separately for several vertical strata. Sometimes the upper and lower heights of the vertical stratum deviate from the definition of the stand layer, e.g. in case of the herb layer. For this layer we found that the height of grasses and forbs often exceeded 0.5 m. Thus, we attributed features up to 1 m to the herb group. Also, some features require a neighbourhood of points outside the stratum for their calculation, in which case the lower height does not start at 0 m. The lidar metrics were grouped into five predictor groups: 1) geometric features as proposed by Weinmann et al. (2015) were used to describe the local 3D shape of the point cloud within a neighbourhood radius of 0.5 and 1 m. We assumed that these features might help to distinguish for example vertically oriented objects like stems from more voluminous objects like shrubs. Nine geometric features based on the eigenvalues and eigenvectors of the 3D structure tensor were calculated. 2) density features such as the number of points in a vertical stratum, either normalised by the total number of points in the vertical column or the number of points within and below the stratum. Such features been used extensively to describe vegetation cover and density in a given layer (Ewald et al., 2014; Campbell et al.,

2018) and have been shown to correlate with fuel load (Skowronski et al., 2007; Bright et al., 2017). 3) intensity information of the lidar returns has been used successfully to filter live (higher intensity returns) and dead tree biomass (lower intensity returns) (Kim et al., 2009) or distinguish live understory components from coarse woody debris (Wing et al., 2012) and could therefore yield information about the presence of different surface fuel components. We did not apply intensity normalisation to our data because elevation differences in our study area were small and only minor improvements were expected according to previous studies (Korpela et al., 2010; You et al., 2017). 4) height metrics were computed to characterise the distribution of returns along the vertical profile of the forest, which has proven useful in previous fuel studies (Jakubowski et al., 2013; Bright et al., 2017; Stefanidou et al., 2020) and 5) voxel metrics derived from voxelisation of the point cloud into 0.5 m cubic voxels were used to capture horizontal variation of point densities within a vertical stratum (e.g. leaf area density as described in Carrasco et al., 2019) to account for potential effects of fuel continuity on fuel loads. Density, intensity, height and voxel metrics were computed in Python 3.8 (van Rossum and Drake, 2009), geometric features were calculated with the Python package 'jakteristics' (Caron and Messal, 2020).

2.5. Multispectral satellite data

We obtained five cloud-free (< 10 % cloud cover) Sentinel-2 scenes as surface reflectance products from five acquisition dates in 2020 (2020-04-04, 2020-05-19, 2020-07-23, 2020-09-21, 2020-11-30). We extracted area-weighted means of the reflectance in the 10 and 20 m bands (bands 2, 3, 4, 5, 6, 7, 8, 8A, 11, 12) from the pixels covering our field plots and additionally calculated a set of spectral indices and biophysical canopy traits using ESA's Sentinel-2 processing toolbox SNAP and Python 3.8 to enhance specific vegetation characteristics. These included leaf area index (LAI), fractional vegetation cover (FCOVER), fraction of absorbed photosynthetically active radiation (FAPAR) (Weiss and Baret, 2016), normalised difference vegetation index (NDVI) (Tucker, 1979), enhanced vegetation index (EVI) (Liu and Huete, 1995), normalised difference moisture index using both SWIR bands 11 and 12 (NDMI, NDMI₂) (Hardisky et al., 1983), soil adjusted vegetation index (SAVI) (Huete, 1988), as well as tasseled cap wetness and greenness (TCW, TCG) (Kauth and Thomas, 1976). A total of 480 lidar metrics and 100 features derived from Sentinel-2 data were calculated, resulting in 580 potential predictors of surface fuel loads, litter and fuelbed depth (Table 4).

2.6. Feature selection

From the 580 calculated features, a pre-selection was made for modelling each surface fuel component. For this purpose, lidar and multispectral predictors were grouped according to their type (geometry, density, intensity, height, voxel, spectral bands, indices) and the forest stand layer for which they were calculated (herb, shrub, canopy; or all stand layers together in the case of height metrics, spectral bands and indices). This resulted in 15 different groups of predictors, e.g. one group would contain only geometric predictors within the herb layer. A pre-selection of two features from each group was conducted to remove redundancy and multicollinearity among predictors by choosing the ones with the highest Spearman correlation with the modelled target and a correlation coefficient < 0.7 between the two features. The set of 30 pre-selected features was further reduced by using the automated "Variable Selection Using Random Forests" (VSURF) algorithm (Genue et al., 2015) in R (v4.2.2, R Core Team, 2022) to obtain a subset optimised for predicting the respective fuel component.

2.7. Random forest modelling

Random forest (RF) regression was chosen to explain the variability

in loads of different surface fuel components across the study area, as the method generally reaches good performance on datasets with a large number of predictors that may have non-linear relationships with the response variable (Breiman, 2001; Strobl et al., 2009). Furthermore, it does not make any formal distributional assumptions about the response variables, which is useful in case of the right-skewed fuel load data, and allows to estimate the importance of different predictor variables. For each fuel component, we trained an RF model on the predictor subset obtained from VSURF using all available samples, and performed a grid search on hyperparameters to optimise the out-of-bag (oob) score of the model and thus reduce overfitting. A new model was trained with the best-scoring hyperparameters and validated using leave-one-out cross-validation (LOOCV). Model performance was evaluated using the coefficient of determination (R^2), root mean squared error (RMSE), relative RMSE (rRMSE) and RMSE normalised with the data range (nRMSE) between random forest predictions and observed fuel load values of the validation data. Our limited sample size of $n = 117-118$ (depending on the fuel component and outliers removed) did not allow an additional hold-out test set; however, RF oob score and cross-validation results showed high agreement and were thus considered reliable estimates of model performance. In addition to the RF model trained on the predictor subset obtained from all predictor types after applying VSURF, we modelled surface fuel loads based on individual predictor types to assess their respective predictive power. For this, we used the pre-selected features from each vertical forest stratum that belonged to the same predictor type, and repeated the VSURF and model training procedure on the new variable subset.

2.8. Comparison of remote sensing-based estimates and average fuel loads

We compared the errors of remote sensing-based continuous fuel load estimates with errors of average fuel loads for different forest types (defined by the dominant overstorey tree species). In this approach, the fuel loads in a field plot were estimated based on the fuel loads in all

other plots of the same forest type. The average of the other plots' fuel loads was taken (separately for each fuel component) and assigned to the plot under consideration, similar to a leave-one-out procedure. RMSE between the forest type-based average values and the observed fuel loads was compared to the RMSE of the RF model based on remote sensing data. Furthermore, we tested for differences in surface fuel loads between forest types defined by dominant tree species using a non-parametric Kruskal-Wallis test (Kruskal and Wallis, 1952) followed by Dunn's test (Dunn, 1964) as post hoc non-parametric test.

2.9. Predictor importance and interpretation

To assess the relevance of the selected variables for predicting the different fuel components, we calculated the permutation feature importance for each feature (Breiman, 2001). This importance metric reveals how much the model relies on a feature by breaking the relationship between feature and target through random permutation of the feature (Molnar, 2022). Additionally, to better understand the relationships between features and modelled target, we computed the accumulated local effect (ALE) of each feature (Apley and Zhu, 2020). ALE gives the relative effect of changing the feature on the prediction within a small interval of the feature. ALE plots are better suited than partial dependence plots to assess the influence of a feature on the prediction when features are correlated (Molnar, 2022). The latter applied to some extent to our dataset even after removing highly correlated features. ALE plots were produced using the python package 'ALEpython' (Jumelle et al., 2020), which allows to create many Monte Carlo replicas by randomly drawing samples from the data and computing ALE on them, thus reflecting its potential variability.

2.10. Surface fuel maps

To obtain fuel load maps at a spatial resolution reflecting the size of our field plots, we resampled the Sentinel-2 data to a pixel size of 14 m

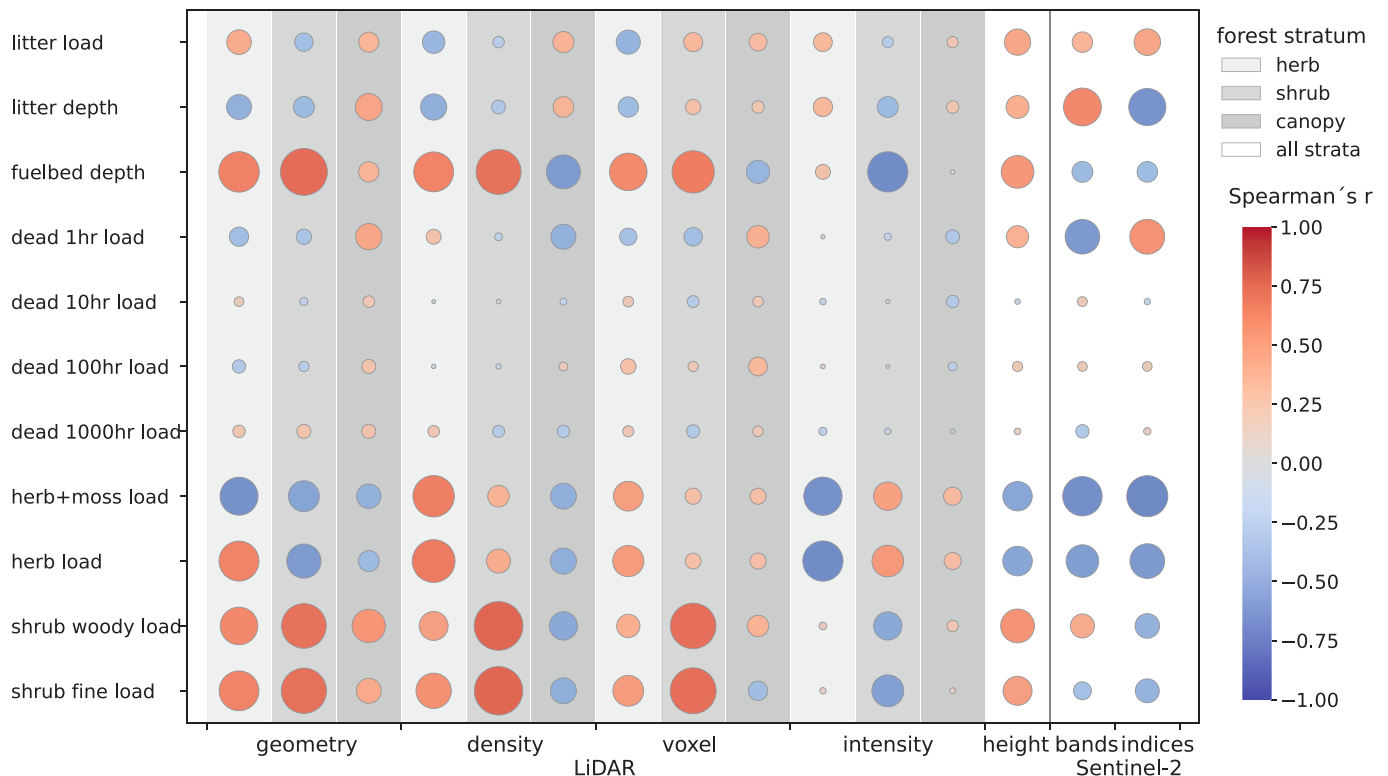


Fig. 3. Highest Spearman correlations of the predictors in each group (defined by forest stratum and predictor type) with the fuel components. Circles are scaled such that the diameters reflect the correlation coefficient, while the column width corresponds to a correlation coefficient of 1.

Table 5

VSURF-selected predictors for the different surface fuel components (omitting 10-1000 hr fuels due to the poor model performance), sorted by their permutation feature importance (first feature has highest importance).

| surface fuel component | predictors |
|------------------------|---|
| litter load | 10th percentile of lidar heights blue reflectance in summer NDVI in summer |
| litter depth | NDVI in early spring 10th percentile of lidar heights FAPAR in autumn |
| fuelbed depth | standard deviation of leaf area density between 1 and 2 m mean omnivariance between 0.5 and 5 m (neighbourhood radius = 1 m) relative point density between 0.5 and 2 m mean return intensity in the herb layer relative point density between 0.5 and 1 m |
| dead 1 hr load | green reflectance in early spring NDWI in early spring SWIR reflectance (2190 nm) in autumn mean planarity between 10 and 15 m (neighbourhood radius = 0.5 m) number of returns in the uppermost meter of the canopy relative to vertical column number of returns in the 5 uppermost meter of the canopy relative to vertical column |
| herb+moss load | NIR reflectance (842 nm) in autumn EVI in autumn number of returns between 0.1 and 0.5 m relative to vertical column coefficient of variation of return intensity in the uppermost meter of the canopy mean linearity between 0.25 and 0.5 m (neighbourhood radius = 0.5 m) skewness of return intensity in the herb layer |
| herb load | coefficient of variation of return intensity in the uppermost meter of the canopy skewness of return intensity in the herb layer number of returns between 0.25 and 0.5 m relative to vertical column EVI in autumn NIR reflectance (842 nm) in autumn |
| shrub woody load | 10th percentile of lidar heights relative point density between 0.5 and 5 m number of non-empty voxels between 2 and 3 m mean linearity between 4 and 5 m (neighbourhood radius = 1 m) mean anisotropy between 0.5 and 5 m (neighbourhood radius = 1 m) mean linearity between 10 and 15 m (neighbourhood radius = 0.5 m) skewness of return intensity between 0.5 and 5 m |
| shrub fine load | mean eigenentropy between 1 and 2 m (neighbourhood radius = 1 m) relative point density between 1 and 2 m mean linearity between 3 and 4 m (neighbourhood radius = 1 m) visible and NIR reflectance (783 nm) in winter mean omnivariance between 0.5 and 1 m (neighbourhood radius = 1 m) coefficient of variation of return intensity between 0.5 and 5 m mean return intensity in the herb layer skewness of lidar heights |

using bilinear interpolation, binned the lidar point cloud into 14 m grid cells, and calculated all features relevant for the predictions for each grid cell. We predicted fuel load maps for the entire study area using the RF models trained on all samples. Fuelbed depth was predicted using separate RF models to ensure meaningful values that matched the spatial patterns of predicted surface fuels. These models were trained based on field-measured loads of the different fuel components. Maps of fuelbed depth were then predicted with these models using the fuel loads from the prediction maps for the individual fuel components created in the preceding step.

2.11. Modelling potential surface fire behaviour

We used spatial predictions of surface fuel loads and fuelbed depth to estimate potential surface fire behaviour in the forest stands of our study area based on the quasi-empirical Rothermel model (Rothermel, 1972). In the underlying basic model, the rate of spread (R in m min^{-1}) of a surface fire through a fuelbed (up to 2 m above the forest floor) is the ratio between the heat flux received (heat source) and the energy required to preheat and ignite the unburned fuel (heat sink) ahead of the fire (Andrews, 2018):

$$R = \frac{\text{heat source}}{\text{heat sink}} = \frac{I_R \xi (1 + \phi_w + \phi_s)}{\rho_b \varepsilon Q_{ig}} \quad (1)$$

Eq. (1) accounts for the effects of wind and slope (ϕ_w, ϕ_s) on the proportion of heat transferred to the fuel (propagating flux ratio ξ) from the energy release at the fire front (reaction intensity I_R in $\text{kJ m}^{-2} \text{s}^{-1}$). The heat required to ignite the fuel depends on the bulk density of the fuel (ρ_b in kg m^{-3} , calculated from load and depth), the proportion of fuel heated to ignition temperature before combustion starts (effective heating number ε) and the heat of preignition (Q_{ig} in kJ kg^{-1}), which is a function of fuel moisture, specific heat of the fuel and assumed ignition temperature (Sandberg et al., 2007; Andrews, 2018). The basic model includes only a single size class of dead fuel, but since surface fuelbeds are a mixture of live and dead fuels of various size classes, the final model includes weighting factors based on the surface area of the fuel in each size class (giving more weight to the finer fuels). Other fire behaviour characteristics commonly modelled are fireline intensity (I_B in $\text{kJ m}^{-1} \text{s}^{-1}$, Eq. 2) as product of reaction intensity (I_R), reaction time (t_r in min) and rate of spread (R), and flame length (F_B in m, Eq. 3) as a function of reaction intensity, both proposed by Byram (1959):

$$I_B = I_R t_r R / 60 \quad (2)$$

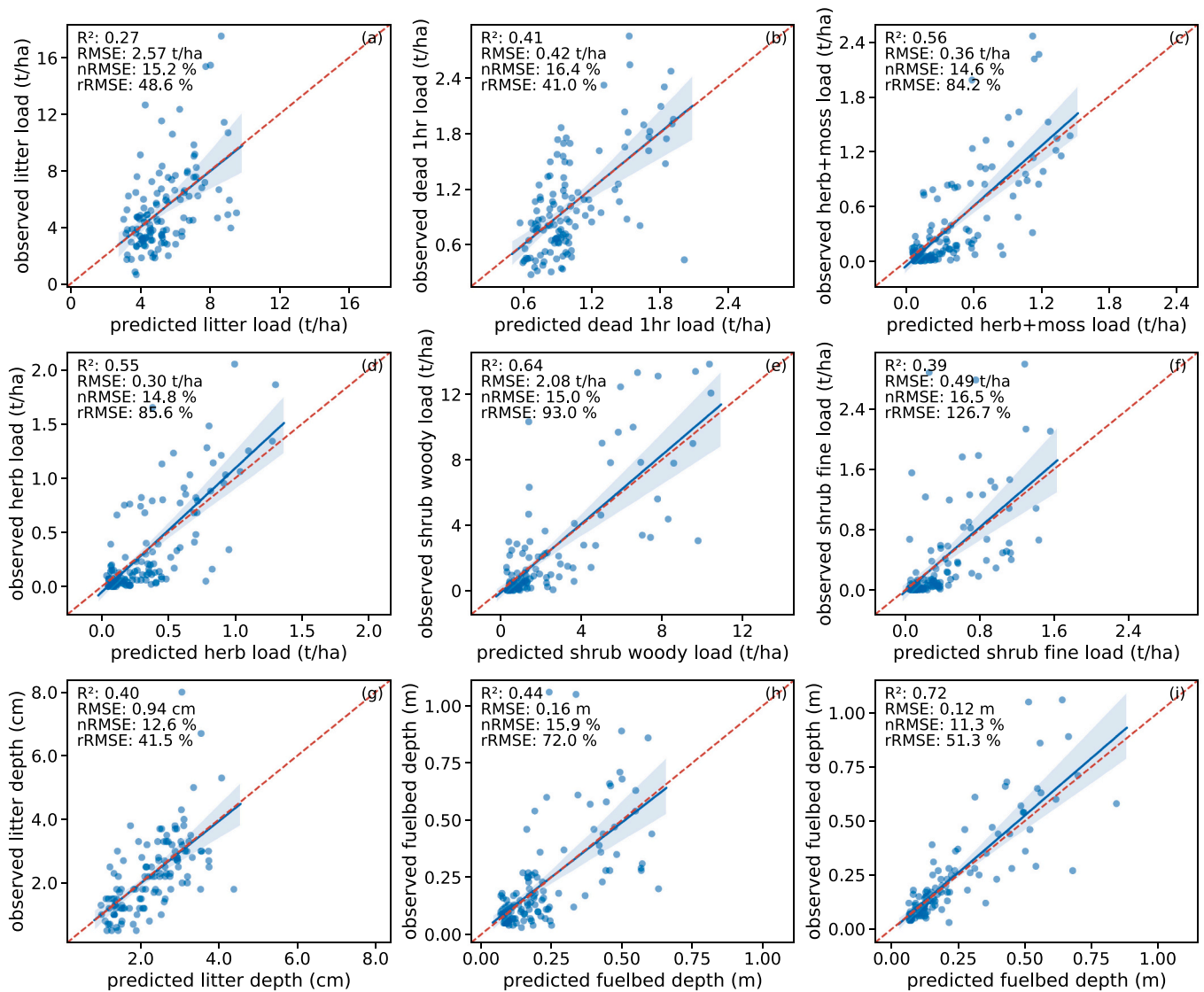


Fig. 4. Scatterplots showing observed (y) and predicted (x) surface fuel loads, litter and fuelbed depth from random forest regression and the model evaluation scores. Blue solid lines show the estimated regression line between predicted and observed values together with the 95% confidence band, the red dashed line is the 1:1 line. Plots h) and i) both show results for fuelbed depth, h) shows the predictions based on remote sensing metrics and i) the predictions based on fuel loads.

Table 6

R^2 and RMSE of models based on predictors of different types. Modelling was omitted if the number of VSURF selected predictors was <2. The best metrics per fuel component are shown in bold.

| | | geometry | density | voxel | intensity | height | all lidar | spectral | all predictor types |
|------------------|-------------|----------|---------|-------|-----------|--------|-------------|----------|---------------------|
| litter load | R^2 | 0.12 | 0.12 | 0.03 | 0.03 | - | 0.13 | 0.15 | 0.27 |
| | RMSE (t/ha) | 2.84 | 2.82 | 3.06 | 3.03 | - | 2.87 | 2.80 | 2.57 |
| dead 1 hr load | R^2 | 0.23 | 0.25 | 0.12 | 0.09 | 0.09 | 0.35 | 0.36 | 0.41 |
| | RMSE (t/ha) | 0.49 | 0.48 | 0.52 | 0.53 | 0.54 | 0.44 | 0.44 | 0.42 |
| herb+moss load | R^2 | 0.47 | 0.38 | 0.30 | 0.27 | 0.14 | 0.53 | 0.41 | 0.56 |
| | RMSE (t/ha) | 0.39 | 0.43 | 0.45 | 0.47 | 0.50 | 0.38 | 0.42 | 0.36 |
| herb load | R^2 | 0.34 | 0.33 | 0.33 | 0.30 | 0.14 | 0.48 | 0.31 | 0.55 |
| | RMSE (t/ha) | 0.37 | 0.37 | 0.37 | 0.38 | 0.43 | 0.33 | 0.38 | 0.30 |
| shrub fine load | R^2 | 0.32 | 0.25 | 0.25 | 0.18 | - | 0.33 | 0.13 | 0.39 |
| | RMSE (t/ha) | 0.53 | 0.55 | 0.55 | 0.57 | - | 0.51 | 0.59 | 0.49 |
| shrub woody load | R^2 | 0.53 | 0.54 | 0.36 | 0.33 | 0.01 | 0.64 | 0.13 | 0.64 |
| | RMSE (t/ha) | 2.38 | 2.33 | 2.79 | 2.83 | 3.43 | 2.08 | 3.24 | 2.08 |
| litter depth | R^2 | 0.22 | 0.16 | 0.05 | 0.08 | - | 0.30 | 0.25 | 0.40 |
| | RMSE (cm) | 1.09 | 1.14 | 1.20 | 1.18 | - | 1.02 | 1.07 | 0.94 |
| fuelbed depth | R^2 | 0.42 | 0.34 | 0.31 | 0.26 | 0.20 | 0.45 | 0.07 | 0.44 |
| | RMSE (m) | 0.17 | 0.18 | 0.18 | 0.19 | 0.20 | 0.16 | 0.22 | 0.16 |

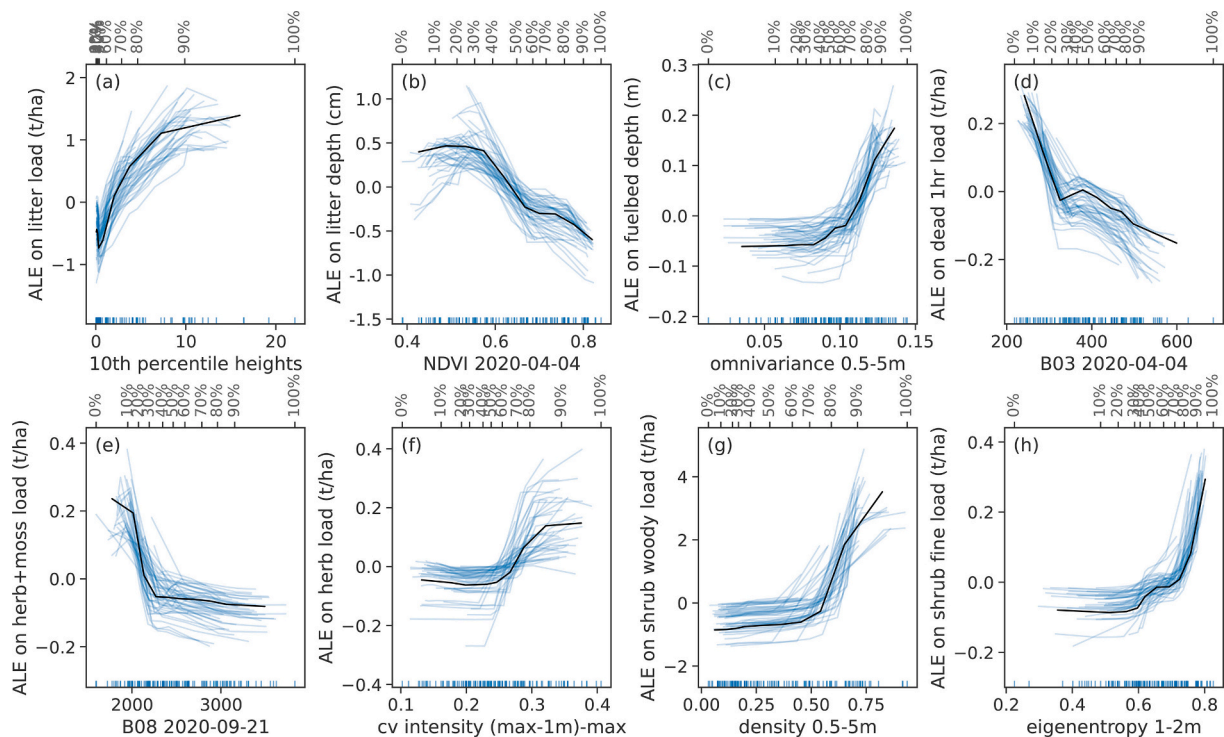


Fig. 5. ALE plots for the most important predictor of each surface fuel component. Effects are centered at zero, which means that an ALE of zero is simply the average prediction and deviations from zero indicate that the prediction is lower/higher than the average prediction by that value. Blue thin lines show the Monte Carlo replicas. Quantiles of the predictor are plotted on the upper axis (percentage values).

$$F_B = 0.45 I_B^{0.46} \tag{3}$$

We used an implementation of the Rothermel equation and related models in R (package ‘firebehaviorR’, Ziegler et al., 2019). All required parameters except fuel loads and fuelbed depth were held constant across the study area and set to the values shown in Table S3 (Supplementary Material). Due to the low performance of our models for the prediction of coarser dead fuels, 10 hr and 100 hr loads were set to the median of all measured values (1.65 and 2.39 t/ha, respectively). Open wind speed was set to 15 km/h and fuel moisture values were based on Scott and Burgan’s (2005) very low fuel moisture scenario D1L1 to reflect severe drought conditions. Fire behaviour characteristics modelled were rate of spread, fireline intensity and flame length.

2.12. Sensitivity analysis

We analysed the sensitivity of the Rothermel model to variations in the different surface fuel components to assess the impact that inaccuracies in fuel load estimation can have on predicted fire behaviour. To this end, we trained a random forest model using the remotely sensed loads of the fine surface fuel components (litter, dead 1 hr, live herbaceous and live fine shrub fuels) across the study area as predictors of the

Table 7

Comparison of RMSE of fuel loads between random forest models based on remotely sensed metrics and predictions based on average values per forest type.

| | RMSE of RF model (t/ha) | RMSE of average fuel loads (t/ha) | error reduction when using RF models (%) |
|--------------|-------------------------|-----------------------------------|--|
| litter | 2.57 | 2.83 | 9 |
| dead 1 hr | 0.42 | 0.45 | 7 |
| herb+moss | 0.36 | 0.50 | 28 |
| herb | 0.30 | 0.44 | 32 |
| shrubs fine | 0.49 | 0.65 | 25 |
| shrubs woody | 2.08 | 3.49 | 40 |

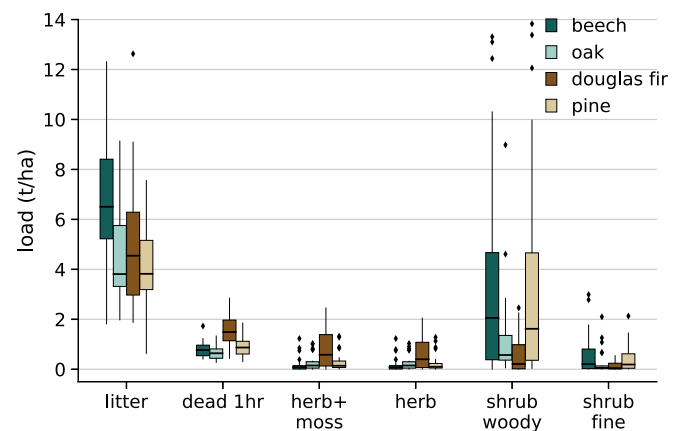


Fig. 6. Loads of surface fuels for the four main forest types. Three outlier points of litter loads are beyond the y-axis range shown.

fire behaviour characteristics calculated with the Rothermel model, thus ensuring realistic combinations of the different fuel components for each instance. We treated each pixel in the study area as an individual sample, since potential fire behaviour is modelled independently of the neighbouring cells. In this way, the random forest model learns the internal relationships and the weighting of the individual fuel components in the Rothermel model and can provide information on which fuel component most strongly influences the predictions. The effect of fuel load variations on predicted fire behaviour characteristics as learned by the random forest model was assessed and visualised using ALE (see chapter 2.9).

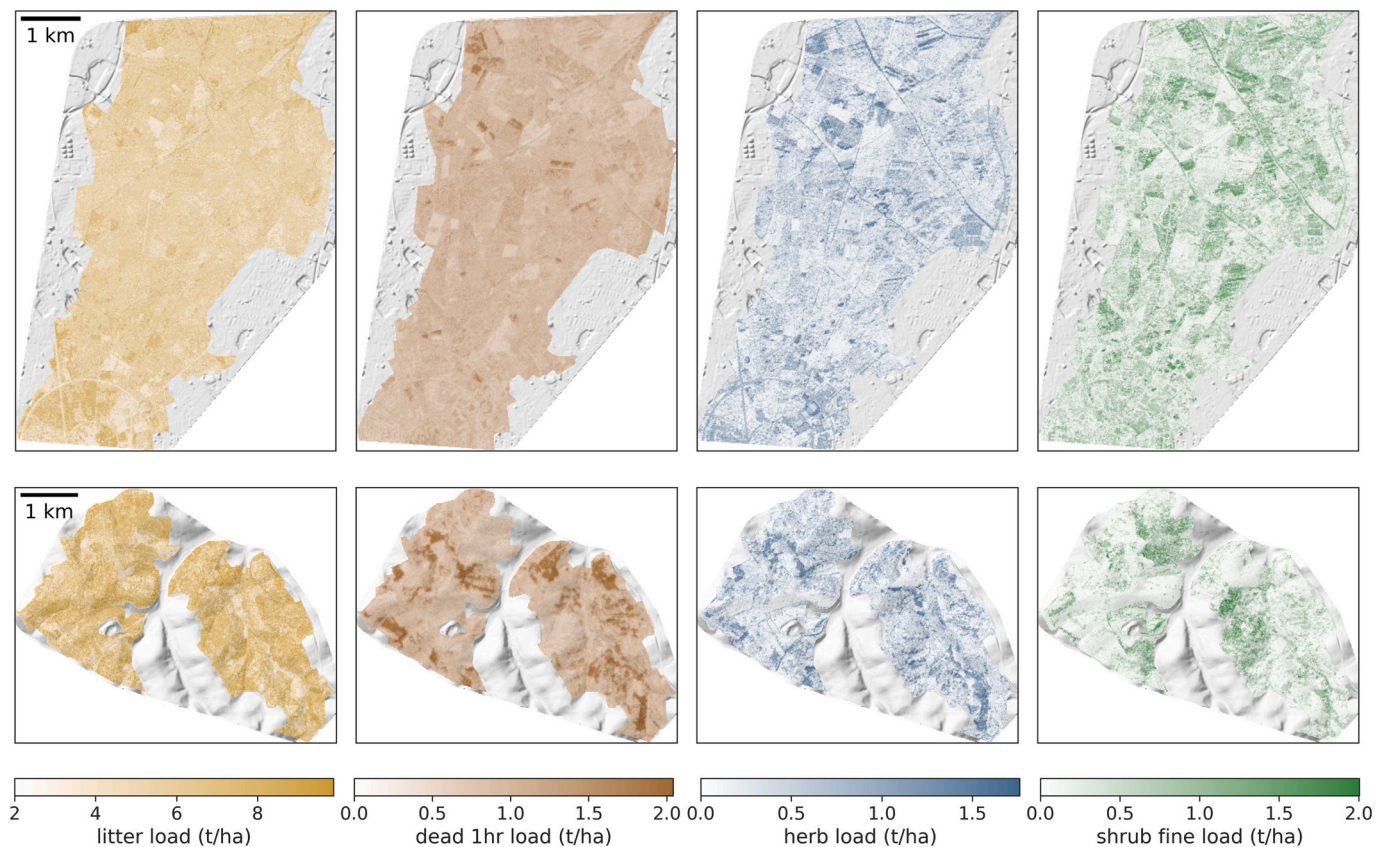


Fig. 7. Predicted fuel load maps on hillshades of the study areas 'Hardtwald' (upper panels) and 'Bretten' (lower panels).

3. Results

3.1. Feature selection

Spearman correlations between field-measured surface fuel components and remotely sensed predictors (Fig. 3) revealed strongest correlations of lidar-derived metrics with understory fuels such as shrubs and herbs, and also fuelbed depth. The most useful lidar metrics for predicting shrub loads were found among geometric, density and voxel features in the corresponding forest stratum. Herb load correlated most strongly with geometric, density and intensity features within the herb layer, but multispectral satellite data also provided information on loads of herbaceous vegetation and mosses. Among the dead woody fuels, only the smallest particle size class (1 hr fuels) showed a notable correlation with multispectral predictors. All coarser dead fuels were not significantly correlated with the predictors, making them difficult to predict using a regression approach. Correlations of litter load and litter depth with the predictors were similarly weak as for dead 1 hr fuels, but were more pronounced for multispectral predictors. After running VSURF on the correlation-based pre-selected feature set (see Table S4 in Supplementary Material), subsets with 3 to 8 variables were obtained for predicting the surface fuel components.

The VSURF-selected features for each surface fuel component are listed in order of their permutation feature importance in Table 5.

3.2. Random forest modelling

Random forest models best explained variation in shrub woody load ($R^2 = 0.64$, Fig. 4 e), while explained variation in shrub fine load was notably lower ($R^2 = 0.39$, Fig. 4 f). Herb load variation was moderately well explained ($R^2 = 0.55$ - 0.56 , Fig. 4 c-d), while model performance for litter and dead 1 hr loads was rather low ($R^2 = 0.27$ and $R^2 = 0.41$, Fig. 4

a-b). RMSE was highest for litter loads (2.57 t/ha), followed by shrub woody loads (2.08 t/ha), while the other fuel components had errors between 0.30 and 0.49 t/ha. The nRMSE was around 15 % for all fuel components, but rRMSE was highest for shrub and herb loads (84.2 % to 126.7 %) due to the many plots with very small fuel loads in these components (Fig. 4 c-f). As expected from the weak correlations between the remotely sensed predictors and the coarser dead fuel loads (10, 100 and 1000 hr fuels, Fig. 3), the RF models explained very little variation ($R^2 = 0.02$ - 0.12) and are not shown here. These fuel components are not included in the further analysis (the 1000 hr fuels are also not considered in Rothermel's fire spread model). Litter and fuelbed depth were modelled with rather low accuracies based on remotely sensed predictors ($R^2 = 0.40$ - 0.44 , Fig. 4 g-h), but fuelbed depth was reasonably well modelled using loads of the different fuel components ($R^2 = 0.72$, Fig. 4 i).

We tested mixed effect random forests and included forest type as a random effect in the model; however, this did not improve the overall results. We also tested a multi-output regression with random forest to predict all surface fuels using a single model, as dependencies between the fuel components are present, albeit weak, but this approach did not improve the results either.

3.3. Results for individual predictor types

Model performance based on individual predictor types (Table 6) reflected the observed patterns of correlation strength (Fig. 3). Results show that modelling surface fuel components benefits from the synergistic use of different predictor types, as models based on variables from all predictor types (described in Table 4) consistently performed best. Results also reveal that stand attributes such as height are insufficient for modelling surface fuel loads and that all other lidar-derived features are mostly relevant for predicting understory fuels rather than litter fuels.

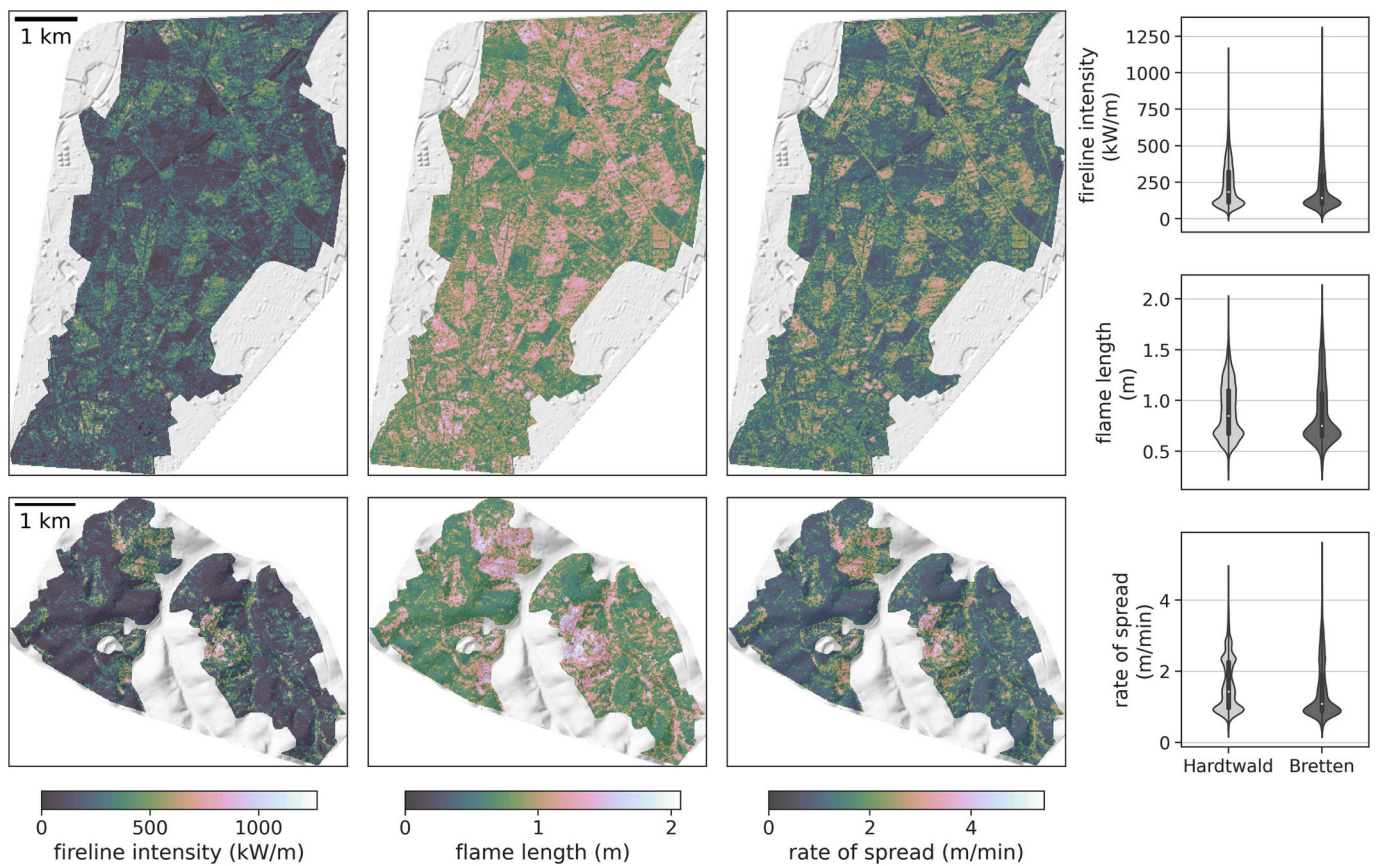


Fig. 8. Potential surface fire behaviour in the study areas as characterised by fireline intensity (left), flame length (middle) and rate of spread (right), and violinplots for the three characteristics per study area. Fire behaviour was calculated assuming 15 km/h open wind speed and extremely low fuel moisture (scenario D1L1, see Scott and Burgan, 2005).

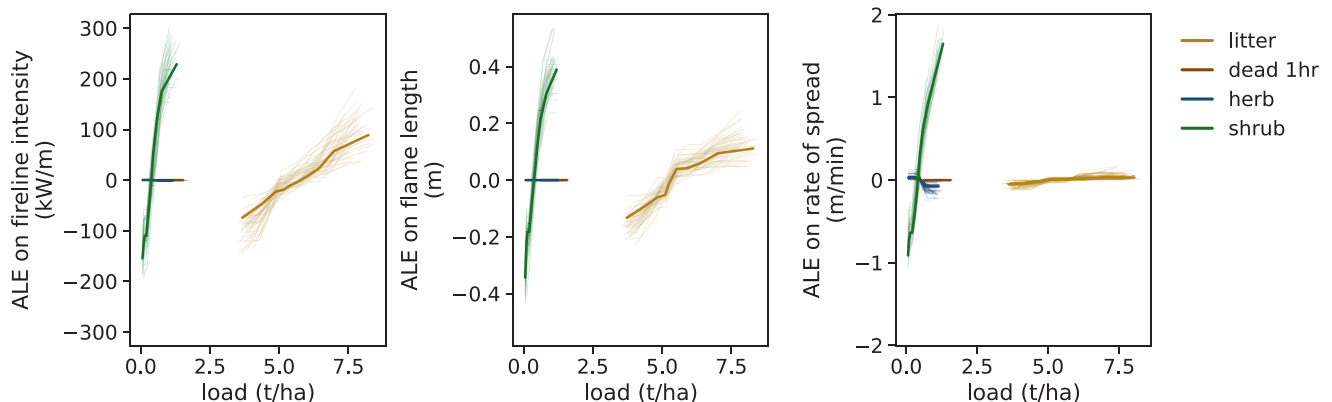


Fig. 9. ALE of surface fuel loads on the fire behaviour characteristics in the study area.

Litter loads are generally the most difficult to model, while models for litter depth are slightly better. Both litter and dead 1 hr fuels benefit from combining lidar and spectral predictors, whereas shrub loads and fuelbed depth are not well predicted from spectral features and rely more on lidar features than from spectral predictors. Herb biomass is slightly better predicted from all lidar features than from spectral predictors, but estimates are improved by combining both. Interestingly, previously unexplored variables such as geometric features have the potential to adequately describe point clouds for fuel mapping, as models based on them sometimes even outperform models based on density features.

3.4. Predictor importance and interpretation

ALE plots are presented and explained for the feature with highest permutation importance (Table 5). Litter loads are predicted using spectral features and the 10th percentile of lidar heights (Fig. 5 a), which describes the height below which 10 % of returns fall: the higher it is, the more returns are found in elevated stand layers, i.e. the canopy, and the lower this value is, the more returns are found near the ground. In the latter case, returns are most likely produced by understory, the presence of which indicates more light penetration and thus a less dense canopy that produces less litter. Litter depth is predicted using similar features and decreases most with higher NDVI in early spring (Fig. 5 b): NDVI at

this time of the year is higher in the younger pine and in the Douglas fir stands of our study area, where understory herbs are developing, and lower in the deciduous beech stands, where highest litter layers accumulate. Fuelbed depth is predicted using lidar features only and increases most with the mean local omnivariance in the shrub layer (0.5 to 5 m) (Fig. 5 c): higher omnivariance corresponds to a more inhomogeneous spread of points over a 3D volume (Waldhauser et al., 2014), indicating the presence of objects with high roughness, such as shrubs or small trees with voluminous structure. Dead 1 hr loads are predicted by spectral rather than lidar features: Reflectance in the green band in early spring is negatively related to predicted loads of dead 1 hr fuels (Fig. 5 d) and lowest reflectance is found in Douglas fir stands, which, due to their crown structure with a high proportion of fine twigs, produce the largest amount of fine dead fuel. The most important features for predicting herb load including mosses are also spectral ones: Predicted loads are higher when reflectance in the NIR band (842 nm) in autumn is lower (Fig. 5 e), which is the case for the coniferous species in the study area. When mosses are excluded from herb biomass, lidar features become more important, but the model still relies on a canopy trait as most important predictor: as the coefficient of variation of lidar return intensity in the uppermost canopy layer increases, modelled herb loads increase (Fig. 5 f). Higher variation in intensity values could be related to the more discontinuous canopy of coniferous trees and less dense canopies in general (e.g. oaks compared to beech), favouring the interaction of the laser beam with different types of surfaces (leaves, exposed branches) of different reflectivity (Kim et al., 2009; Fassnacht et al., 2016). Shrub loads are modelled using lidar features only: While shrub woody loads increase with mean point density in the layer between 0.5 and 5 m (Fig. 5 g), the model for fire-relevant shrub fine load is more sensitive to returns between 1 and 2 m (Fig. 5 h), which corresponds to the requirement to stay within 2 m above the forest floor. The higher the eigenentropy of the point cloud in this layer, i.e. the higher the disorder of points, the more fine shrub material is predicted.

3.5. Comparison of remote sensing-based estimates and average fuel loads

Comparison between errors of the remote sensing-based fuel load estimates and errors of the average fuel load estimates based on the four main forest types (Table 7) shows that canopy-related fuels such as litter and dead 1 hr fuels can be predicted with comparable accuracy by forest type alone. In our study area, litter loads were significantly higher in beech stands than oak, Douglas fir and pine stands, while dead 1 hr loads were significantly higher in Douglas fir stands compared to pine, beech and oak stands (Fig. 6). Understory vegetation was predicted with lower RMSE using the remote sensing-based models compared to forest type-based predictions. Maximum error reduction (40 %) using the RF model based on remote sensing data was achieved for shrub woody load (Table 7). In our study area, differences in herb load (both with and without moss) and shrub load between forest types were small. Significant differences were only found in herb load between Douglas fir and beech stands and in shrub woody load between Douglas fir and beech or pine stands. Shrub fine biomass was significantly higher only in pine stands compared to Douglas fir stands (Fig. 6).

3.6. Surface fuel maps

Maps are shown for fuel components that have the greatest influence on surface fire behaviour, i.e., the fine dead and live fuels (Fig. 7). Litter load ranges from 2.8 to 9.9 t/ha in the study areas, with higher mean and variance (6.4 ± 1.3 t/ha) in *Bretten* compared to *Hardtwald* (5.2 ± 0.9 t/ha). Dead 1 hr load varies between 0.5 and 2.0 t/ha and is again slightly higher and more variable in *Bretten* (1.0 ± 0.3 t/ha) than in *Hardtwald* (0.9 ± 0.2 t/ha). Herb load ranges from 0 to 1.8 t/ha with similar mean and variance (0.4 ± 0.3 t/ha) in both study areas. Fine shrub load ranges between 0 and 2.0 t/ha and is lower on average in *Bretten* (0.4 t/ha) than in *Hardtwald* (0.5 t/ha), but equally variable (± 0.3 t/ha).

3.7. Potential surface fire behaviour

Surface fires are predicted to have low intensity in large parts of the study area (mean fireline intensity: 228 kW/m) under the given parametrisation of physical fuel properties, moisture and wind speed (

Fig. 8). The highest fireline intensity (1269 kW/m) can be found in a part of the eastern *Bretten* forest, where predicted flame length and spread rate also show maximum values (2.1 m and 5.4 m/min, respectively). Mean potential flame length for the study areas is 0.9 m, and mean rate of spread is 1.6 m/min. All three fire behaviour characteristics show similar patterns across the study areas and suggest a high correlation with the underlying fuel load patterns.

3.8. Sensitivity analysis

Examining the effects of individual fuel components on modelled fire behaviour characteristics using a random forest model ($R^2=0.92-0.96$ on independent test set, Figure S5 in Supplementary Material) reveals that shrub load has by far the highest influence on the modelled output, despite the small range of values in the study area, as indicated by the steepness of the ALE curve (Fig. 9). All fire behaviour characteristics become more severe with increasing shrub load, while dead 1 hr fuels and herb fuels seem to have a negligible effect. Increasing litter load also leads to higher modelled intensities and flame lengths, while the effect on spread rate is minor. Errors in shrub and litter load predictions thus have the greatest impact on modelled potential fire behaviour and underestimated loads in particular can lead to severely underestimated fire behaviour. Figure S6 (Supplementary Material) shows how modelled fire behaviour in the study areas changes when loads of fine shrub and litter fuels are both increased by their model RMSE (0.49 t/ha and 2.57 t/ha, respectively, and fuelbed depth adjusted accordingly).

4. Discussion

4.1. Potential and limitation of surface fuel load predictions using remote sensing

Our results show that random forest regression models based on lidar and multispectral variables describing forest composition and structure are able to predict loads of surface fuel components in heterogeneous mixed forests of Central Europe with moderate to low accuracy.

4.2. Litter and fine woody fuels

Consistent with previous studies from different ecosystems (e.g. Jakubowski et al., 2013; Bright et al., 2017; Alonso-Rego et al., 2021), ground-based fuels such as litter and deadwood were the most difficult to estimate accurately from remote sensing data. We found that the variability in litter and dead 1 hr loads was mostly explained by remotely sensed predictors capturing canopy properties, rather than by lidar reflections near the ground itself, and that the accuracy of the predictions was generally low. A possible reason for this is that litter and fine woody fuels (dead 1 hr) can vary at centimeter scales depending on the micro-topography of the forest floor, the presence of herbaceous plants and mosses, or fallen branches under which especially dead needles and fine twigs accumulate. This heterogeneity may not be adequately represented in the field data, and additionally airborne lidar data were probably not fully capable of capturing this variation, both of which add uncertainty. Previous studies have shown that even with terrestrial laser scanning it is not possible to obtain information on litter or 1 hr fuel loads with sufficient accuracy (Arkin et al., 2023). Our results indicate that the captured variability in litter and fine woody fuels is mostly explained by differences in litter and fine fuel production between different tree species and canopy densities, which are reflected in the multispectral data. However, the low observed accuracies suggest that litter and 1 hr fuel loads are determined by additional factors that

cannot be captured with the remote sensing data used. For example, litter loads are closely linked to decomposition rates, which depend not only on litter chemistry but also on temperature and humidity, soil conditions and microbial activity (Krishna and Mohan, 2017) and are therefore related to the general site conditions. As fuel sampling was performed from May to October in two consecutive years, different stages of litter decomposition may have added further variability to the data. We also sometimes found leaf litter from neighbouring trees blown into our field plots. The comparable error when using average fuel loads based on forest types suggests that detailed remote sensing data provide only little added value in predicting litter and 1 hr fuel loads. This is in line with the finding of Alonso-Rego et al. (2021), who report as little as 10 % variance explained in litter and duff loads of pure even-aged pine stands based on ALS metrics, and those of Bright et al. (2017), who explain 16 % (24 %) of variation in litter and duff loads using ALS only (in combination with disturbance-related metrics derived from Landsat time series), and 21 % (28 %) in 1–100 hr fuels in a study area with multiple coniferous species. However, it is contrasting the findings of Stefanidou et al. (2020), who explain 69 % of variation in litter loads and 59 % in dead 1 hr loads using multispectral lidar in a study area with pure fir overstory and suggest that lidar is interacting with the litter fuels in a direct manner. One reason for the rather low accuracies in our study may be the structurally and compositionally complex forest stands, making it difficult to disentangle the different drivers (e.g. tree species, age and stand or canopy density) of measured fine fuel loads at the forest floor, unless these relationships are studied based on a substantially larger dataset. Our study suggests that in such cases, multispectral remote sensing data that allow reliable classification of forest types can be considered the most efficient option for predicting litter and fine woody fuel components through association with average loads that need to be determined for a forest type and site, even though this method has limited accuracy. The forest type-specific fuel loads could be refined by either coupling them with a biophysical model predicting rates of fine fuel accumulation and decomposition throughout the year (e.g., Hanan et al., 2022), or an empirically derived model that links seasonal variations in fine fuel loads to remotely sensed phenological variations in trees (e.g., Zeilhofer et al., 2012).

4.2.1. Coarse woody fuels

For the coarser dead fuels, we could not develop a model that was able to explain the variation in loads. While Jakubowski et al. (2013) similarly reported little correlation between ALS metrics and 1000 hr fuels, Bright et al. (2017) explained 30 % variance in 1000 hr loads based on ALS metrics only and 32 % in combination with Landsat-derived disturbance metrics, and Alonso-Rego et al. (2021) reported 41 % variance explained in combined woody debris load using ALS. Combined estimates were not made in our study, and the weak results for the individual woody fuel components can be explained by the variability and many zeros in the observed loads in our study area, especially for the coarsest particle size class of the 1000 hr fuels, for which the calculated loads depend strongly on the geometry of the lying stems (diameter and length). Furthermore, the occurrence of these fuel particles is highly heterogeneous both within a field plot and in the entire forest stand. The field plot size thus influences the fuel variability captured, and additionally determines the sensitivity to registration errors between field plots and lidar or satellite data (especially when only few pixels overlap with the field plots, as in our case). Due to the heterogeneous distribution of downed wood, detecting logs in high-resolution optical imagery (preferably acquired from below canopies) or lidar point clouds and then determining the volume of the individual logs, as has been done successfully by e.g. Lopes Queiroz et al. (2020) and Jarron et al. (2021), would be better suited to approximate loads. Accurate localisations of lying logs may actually be more useful for fine-scale fire behaviour analyses and for assessing the accessibility of forest areas for firefighting, but fuel models for spatial fire applications still include area-based loads for coarse fuels. However, a manual

examination of our lidar point cloud suggested that in heterogeneous stands with understory presence, even large logs are difficult to resolve and lidar penetration to the ground is sometimes significantly reduced depending on canopy density. Also 10 hr (0.63–2.54 cm diameter) and 100 hr (2.55–7.62 cm diameter) fuel loads are difficult to map, which is not surprising given the relatively large footprint of several centimeters in airborne lidar acquisitions. But even with terrestrial lidar, it is difficult to quantify loads of 10 hr and 100 hr fuels (Arkin et al., 2023). Lastly, the amount of coarse dead fuels is less predictable by tree species composition than litter and dead 1 hr fuels: their occurrence is more random as it depends on forest management activities such as logging and pruning or natural disturbance such as windthrow and falling branches after strong winds or heavy snowfall. Mortality can also be influenced by different soil conditions, which affect a tree's susceptibility to drought. In our case, the time lag between lidar acquisition and field measurements might have further affected the prediction, as interventions such as removal of deadwood or accumulation of branches after strong winds might not have been recorded in one of the datasets. Remote sensing can help identify major disturbance events and detect trees that may become deadwood sources after insect infestation or drought (Brodrick and Asner, 2017; Kislov et al., 2021), but accurate quantification of accumulating woody debris at the forest floor remains challenging and especially management effects will be difficult to account for as long as no direct and timely detection of deadwood is possible.

4.2.2. Herb and moss fuels

Understory fuel load in the herb layer was moderately well predicted using our RF models. Prediction of moss and herb fuels relied mostly on multispectral features (Table 5), as their occurrence in our study area is strongly biased towards conifer stands, which contrast strongly with broadleaved stands in the spectral domain. As expected, information on canopy characteristics was helpful in predicting herbaceous fuel loads, because canopy composition and density control the amount of light reaching the forest floor. Tree cover alone, as reflected in the lidar metrics and also estimated in the field, was not as strongly correlated with herbaceous fuel loads as the multispectral features. However, structural information from below the canopy obtained from lidar data was also useful and gained importance when herbaceous biomass was predicted independently of mosses. The variance explained with our herb load model was similar to what is reported in a study predicting herbaceous cover from airborne lidar in temperate forests (Latifi et al., 2017), but despite the high point density of our dataset, we could not reach the performance of models based on TLS-derived metrics (Wallace et al., 2017; Li et al., 2021). As biomass does not only depend on cover, but also on plant height and bulk density and thus on the type of understory vegetation or more specifically the species present (Bolte, 2006), these metrics need to be estimated precisely, which is unlikely to be achieved based on ALS. But even if the vegetation volume of the herb layer cannot be derived as accurately as from TLS point clouds, ALS-derived cover (and height) estimates may still allow to approximate biomass if species information is available. Such information could be derived from existing knowledge of herbaceous plant communities that develop under specific site conditions, and should take into account seasonal variations in their composition and condition (e.g., spring flowering and senescence). Our data showed that there was a slightly decreasing trend in measured herbaceous biomass over the year (Spearman $r = -0.42$), which is important to consider for dynamic fuel estimates. Despite limitations, models based on remotely sensed structural and spectral metrics can improve the prediction of herbaceous loads compared to predictions based on forest types alone.

4.2.3. Shrub fuels

Shrub fuel load predictions relied almost exclusively on lidar metrics and provided reasonable accuracy for shrub woody loads, but poorer results for the more fire model-relevant fine biomass. Shrub load is

species-dependent like herb load and additionally determined by wood density (Annighöfer et al., 2016), and therefore not perfectly correlated with cover and/or height extracted at plot-level. While shrub cover has been well predicted from airborne lidar point clouds (Wing et al., 2012), difficulties in estimating shrub height from lidar have been reported when different shrub species are present (Alonso-Rego et al., 2021). Having included geometric features as descriptors of point cloud shape in our study may not have been sufficient to account for the effects of different growth forms on biomass. However, these features may still offer potential for improving approaches to understory species segmentation (e.g., Wang, 2020) as basis for developing species-specific biomass models from point cloud data. Additionally, geometric features have been successfully applied in leaf-wood classifications of forest point clouds (Krishna Moorthy et al., 2020) and could serve to separate the fire model-relevant fine shrub load in this way. We also acknowledge that our reference shrub load data are subject to considerable uncertainty: their accuracy is limited by the availability of accurate allometric equations for calculating biomass from diameter at stem base (DAB), and by the accuracy of the biomass partitioning into different plant compartments used to estimate fine biomass in our study (see Supplementary Material S1). It is also well known that growth morphology of understory trees and shrubs, even of the same species, changes with light conditions: In our study area, despite having the same DAB, young beech trees in particular either had long stems with branches and leaves located further from the ground or remained rather small depending on light availability. This has an important impact on the biomass available near the ground that can burn in a surface fire. In addition, in a few cases there were still branches of mature trees in the surface fuel layer, but these were not included in the measurement of shrub fuels. The only way to avoid this uncertainty is to collect all the shrub material within the fire relevant layer and sort it by particle size, which is often not feasible due to time and personnel constraints. Alternatively, existing approaches to characterise shrubs from dense point clouds acquired with terrestrial laser scanning (e.g. Hudak et al., 2020; Li et al., 2021) could be used to calibrate better models for shrub woody and fine biomass. Overall, the inclusion of detailed structural information derived from airborne lidar was more relevant for the prediction of shrub fuel loads than for any other fuel component, and this approach should be favoured over assigning average fuel loads based on forest types. The same is true for the closely related fuelbed depth if it is not estimated from the fuel loads themselves.

4.3. Surface fuel maps and potential surface fire behaviour

Despite the limited performance of the remote sensing-based models, the generated fuel load maps show clear patterns that match field observations of the respective fuel components and can thus inform forest managers and firefighters about the fuel situation at a fine scale. Modelled potential fire behaviour remains unvalidated due to lack of reference data from real fires in the study area. However, our results were broadly consistent with the findings of Heisig et al. (2022), who reported similar surface fuel load ranges in a study area dominated by Scots pine, European beech and red oak in northwestern Germany, and modelled fire behaviour under different environmental conditions. They used constant fuel loads depending on forest type and found the spatial patterns of fire behaviour to be closely linked to those of the surface fuel models. Under the same moisture scenario and a wind speed half of ours, they simulated a mean spread rate of 2.6 m/min and flame length of 2.5 m, which is about twice as high as our values. Considering the known difficulty of predicting realistic fire behaviour based on actual fuel loads (Burgan, 1987), we conclude that the absolute values should be treated with caution. Nevertheless, we assessed how errors in fuel load estimates affect predicted fire behaviour through the mechanistic relationships in the Rothermel model and found that errors in shrub load have the strongest effect, followed by litter load. This is most likely due to the effect of the presence of shrubs on fuelbed depth, which strongly impacts

bulk density of the fuelbed and thus changes the estimated rate of spread and associated fire characteristics. We also noted that the assumption of the Rothermel model that fuel particles are homogeneously distributed over the fuelbed was not fulfilled in our study: bulk density decreased from the bottom of the litter layer to the top of the fuelbed, but this was not reflected in the averaged fuelbed depth and bulk density, which probably led to underestimated fire spread rates (Cruz and Fernandes, 2008). The remarkable effect of litter load on fireline intensity and flame length is due to its influence on reaction intensity, which is a function of net fuel load (Andrews, 2018), of which litter is the largest component in this study. As the two most influential fuel components were at the same time associated with the highest prediction error in our models, we recommend that future research on surface fuels in temperate forests should focus on improving estimates of litter and shrub fuel loads, as well as fuelbed depth.

5. Conclusion

Statistical relationships between remotely sensed metrics describing forest composition and structure and surface fuels have some potential for estimating fuel loads in Central European forest types. Still, we confirm previous studies in other ecosystems that establishing robust relationships is challenging. Random forest regression based on multiple spectral and structural characteristics derived from airborne lidar and multispectral satellite data showed that a combination of different metric types is most useful for fuel load estimation. It also revealed that previously unexplored metrics such as geometric features calculated from lidar point clouds may be an interesting alternative to the more commonly used density-related metrics. Multispectral information is most useful for estimating canopy-related fuels such as litter and dead 1 hr fuels, but can also be linked to other relevant stand properties, such as the presence of mosses under certain tree species. Multispectral information in combination with lidar helps to estimate herb fuels, while shrub fuels can be estimated with lidar alone, and results can probably be improved by developing adequate biomass models from selected metrics. Dead woody fuels are difficult to relate to metrics aggregated at field plot level and may be better captured with object-based approaches on TLS or photogrammetric data. The data-driven regression approach and feature-selection process employed in this study are efficient; however, the application of more sophisticated (point cloud) processing methods targeting the individual fuel components and their spatial scale of variation may help to improve the estimates. For dynamic fuel load estimates, ecological processes and knowledge of management and disturbance events must also be included. Extending the method to larger areas is limited by the availability of high-resolution airborne lidar data, but spaceborne lidar data from instruments such as GEDI and spaceborne radar data could be a possible substitute that needs further research. In general, remote sensing-based fuel load predictions were more accurate than average fuel loads based on forest type. However, the latter can be sufficient for fuel components that are relatively constant underneath a certain tree species at a certain site, e.g. litter and dead 1 hr fuels. Understory fuels and fuelbed depth, in contrast, should be estimated at finer scales, preferably using structural information derived from lidar. This is important given their strong influence on fire dynamics, which is also reflected in the high sensitivity of fire behaviour models to variations in understory, particularly shrub fuel loads.

Author statement

Pia Labenski: Conceptualization, Data acquisition, Methodology, Formal analysis, Writing – Original Draft. Michael Ewald: Conceptualization, Data acquisition, Writing – Review & Editing. Sebastian Schmidlein: Writing – Review & Editing. Faith Ann Heinsch: Writing – Review & Editing. Fabian Ewald Fassnacht: Conceptualization, Writing – Review & Editing, Supervision, Funding acquisition.

Declaration of Competing Interest

The authors declare that they have no known competing financial interests or personal relationships that could have appeared to influence the work reported in this paper.

Data availability

Data will be made available on request.

Acknowledgements

This work was funded by the German Federal Ministry of Food and Agriculture and Federal Ministry for the Environment, Nature Conservation and Nuclear Safety as part of the project “ErWiN” (code 2219WK54A4). We would like to thank the anonymous reviewers for their valuable comments and suggestions to improve this manuscript.

Appendix A. Supplementary material

Supplementary data to this article can be found online at <https://doi.org/10.1016/j.rse.2023.113711>.

References

- Albini, F.A., 1984. Wildland Fires: Predicting the behavior of wildland fires—among nature’s most potent forces—can save lives, money, and natural resources. *Am. Sci.* 72 (6), 590–597.
- Alonso-Rego, C., Arellano-Pérez, S., Guerra-Hernández, J., Molina-Valero, J.A., Martínez-Calvo, A., Pérez-Cruzado, C., Castedo-Dorado, F., González-Ferreiro, E., Álvarez-González, J.G., Ruiz-González, A.D., 2021. Estimating stand and fire-related surface and canopy fuel variables in pine stands using low-density airborne and single-scan terrestrial laser scanning data. *Remote Sens.* 13 (24), 5170.
- Andersen, H.-E., McGaughey, R.J., Reutebuch, S.E., 2005. Estimating forest canopy fuel parameters using LIDAR data. *Remote Sens. Environ.* 94 (4), 441–449.
- Andrews, P.L., 2018. The Rothermel surface fire spread model and associated developments: A comprehensive explanation. Gen. Tech. Rep. RMRS-GTR-371. U.S. Department of Agriculture, Forest Service, Rocky Mountain Research Station, Fort Collins, CO, 121 p. 371.
- Annighöfer, P., Ameztegui, A., Ammer, C., Balandier, P., Bartsch, N., Bolte, A., Coll, L., Collet, C., Ewald, J., Frischbier, N., Geberyesus, T., Haase, J., Hamm, T., Hirschfelder, B., Huth, F., Kändler, G., Kahl, A., Kawaletz, H., Kuehne, C., Lacoïnte, A., Lin, N., Löf, M., Malagoli, P., Marquier, A., Müller, S., Promberger, S., Provendier, D., Röhle, H., Sathornkitch, J., Schall, P., Scherer-Lorenzen, M., Schröder, J., Seele, C., Weidig, J., Wirth, C., Wolf, H., Wollmerstädt, J., Mund, M., 2016. Species-specific and generic biomass equations for seedlings and saplings of European tree species. *Eur. J. Forest Res.* 135 (2), 313–329.
- Apley, D.W., Zhu, J., 2020. Visualizing the effects of predictor variables in black box supervised learning models. *J. R. Stat. Soc. B* 82 (4), 1059–1086.
- Arellano-Pérez, S., Castedo-Dorado, F., López-Sánchez, C., González-Ferreiro, E., Yang, Z., Díaz-Varela, R., Álvarez-González, J., Vega, J., Ruiz-González, A., 2018. Potential of Sentinel-2A data to model surface and canopy fuel characteristics in relation to crown fire hazard. *Remote Sens.* 10 (10), 1645.
- Arkin, J., Coops, N.C., Daniels, L.D., Plowright, A., 2023. Canopy and surface fuel estimations using RPAS and ground-based point clouds. *Forestry*, cpad020. <https://doi.org/10.1093/forestry/cpad020>.
- Battisti, C., Poeta, G., Fanelli, G., 2016. An introduction to disturbance ecology. In: A Road Map for Wildlife Management and Conservation.
- Bolte, A., 2006. Biomasse- und Elementvorräte der Bodenvegetation auf Flächen des forstlichen Umweltmonitorings in Rheinland-Pfalz. Institut für Waldbau, Universität Göttingen, Berichte des Forschungszentrum Waldökosysteme.
- Botequim, B., Fernandes, P.M., Borges, J.G., González-Ferreiro, E., Guerra-Hernández, J., 2019. Improving silvicultural practices for Mediterranean forests through fire behaviour modelling using LiDAR-derived canopy fuel characteristics. *Int. J. Wildland Fire* 28 (11), 823–839.
- Brandis, K., Jacobson, C., 2003. Estimation of vegetative fuel loads using Landsat TM imagery in New South Wales, Australia. *Int. J. Wildland Fire* 12 (2), 185.
- Breiman, L., 2001. Random Forests. *Mach. Learn.* 45 (1), 5–32.
- Bright, B., Hudak, A., Meddens, A., Hawbaker, T., Briggs, J., Kennedy, R., 2017. Prediction of forest canopy and surface fuels from lidar and satellite time series data in a bark beetle-affected forest. *Forests* 8 (9), 322.
- Brodrick, P.G., Asner, G.P., 2017. Remotely sensed predictors of conifer tree mortality during severe drought. *Environ. Res. Lett.* 12 (11), 115013.
- Burgan, R.E., 1987. Concepts and Interpreted Examples in Advanced Fuel Modeling. U.S. Department of Agriculture, Forest Service, Intermountain Research Station (en).
- Burgan, R.E., Rothermel, R.C., 1984. BEHAVE. Fire Behavior Prediction and Fuel Modeling System, Fuel Subsystem. Intermountain Forest and Range Experiment Station, Forest Service, U.S. Department of Agriculture (en).
- Byram, G.M., 1959. Combustion of forest fuels. *Forest. Fire* 61–89.
- Campbell, M.J., Dennison, P.E., Hudak, A.T., Parham, L.M., Butler, B.W., 2018. Quantifying understory vegetation density using small-footprint airborne lidar. *Remote Sens. Environ.* 215, 330–342.
- Caron, D., Messal, L., 2020. jakteristics, GitHub repository.
- Carrasco, L., Giam, X., Papeş, M., Sheldon, K., 2019. Metrics of lidar-derived 3D vegetation structure reveal contrasting effects of horizontal and vertical forest heterogeneity on bird species richness. *Remote Sens.* 11 (7), 743.
- Chen, Y., Zhu, X., Yebra, M., Harris, S., Tapper, N., 2017. Development of a predictive model for estimating forest surface fuel load in Australian eucalypt forests with LiDAR data. *Environ. Model. Softw.* 97, 61–71.
- Chirici, G., Scotti, R., Montagni, A., Barbat, A., Cartisano, R., Lopez, G., Marchetti, M., McRoberts, R.E., Olsson, H., Corona, P., 2013. Stochastic gradient boosting classification trees for forest fuel types mapping through airborne laser scanning and IRS LISS-III imagery. *Int. J. Appl. Earth Obs. Geoinf.* 25, 87–97.
- Cruz, M.G., Fernandes, P.M., 2008. Development of fuel models for fire behaviour prediction in maritime pine (*Pinus pinaster* Ait.) stands. *Int. J. Wildland Fire* 17 (2), 194.
- Dell, J.E., Richards, L.A., O’Brien, J.J., Loudermilk, E.L., Hudak, A.T., Pokswinski, S.M., Bright, B.C., Hiers, J.K., Williams, B.W., Dyer, L.A., 2017. Overstory-derived surface fuels mediate plant species diversity in frequently burned longleaf pine forests. *Ecosphere* 8 (10), e01964.
- Domingo, D., La Riva, J., Lamelas, M.T., García-Martín, A., Ibarra, P., Echeverría, M., Hoffrén, R., 2020. Fuel type classification using airborne laser scanning and Sentinel 2 data in mediterranean forest affected by wildfires. *Remote Sens.* 12 (21), 3660.
- Duff, T.J., Bell, T.L., York, A., 2013. Predicting continuous variation in forest fuel load using biophysical models: a case study in south-eastern Australia. *Int. J. Wildland Fire* 22 (3), 318.
- Dunn, O.J., 1964. Multiple comparisons using rank sums. *Technometrics* 6 (3), 241–252.
- DWD Climate Data Center, 2023. Historical monthly station observations (temperature, precipitation, sunshine duration, wind and cloud cover) for Germany, Version v22.3 urn:x-wmo:md:de.dwd.cdc:obsgermany-climate-monthly-kl-historical.
- EFFIS, 2023a. European Forest Fire Information System - Statistics Portal. European Commission. <https://effis.jrc.ec.europa.eu/apps/effis.statistics/estimates>. Accessed 24 January 2023.
- EFFIS, 2023b. European Forest Fire Information System - Current Situation Viewer. European Commission. https://effis.jrc.ec.europa.eu/apps/effis_current_situation/. Accessed 24 May 2023.
- Elmqvist, M., Jungert, E., Lantz, F., Persson, A., Soderman, U., 2001. Terrain modelling and analysis using laser scanner data. *Int. Arch. Photogramm. Remote Sens. Spat. Inf. Sci.* 34 (3), 219–226.
- Ewald, M., Dupke, C., Heurich, M., Müller, J., Reineking, B., 2014. LiDAR remote sensing of forest structure and GPS telemetry data provide insights on winter habitat selection of European Roe Deer. *Forests* 5 (6), 1374–1390.
- Fassnacht, F.E., Latifi, H., Stereńczak, K., Modzelewska, A., Lefsky, M., Waser, L.T., Straub, C., Ghosh, A., 2016. Review of studies on tree species classification from remotely sensed data. *Remote Sens. Environ.* 186, 64–87.
- Finney, M.A., 2006. An overview of flammability fire modeling capabilities. In: *Fuels Management - How to Measure Success: Conference Proceedings*, pp. 213–220.
- ForstBW, 2019. Waldentwicklungstypenkarte. Gemeinde Walzbachtal, Landkreis Karlsruhe, Untere Forstbehörde.
- ForstBW, 2023. Geo-Daten: Waldeinteilung. <https://www.forstbw.de/produkte-angebote/geo-daten/>. Accessed 23 May 2023.
- Fosberg, M.A., Lancaster, J.W., Schroeder, M.J., 1970. Fuel moisture response—drying relationships under standard and field conditions. *For. Sci.* 16 (1), 121–128.
- Franke, J., Barradas, A.C.S., Borges, M.A., Menezes Costa, M., Dias, P.A., Hoffmann, A.A., Orozco Filho, J.C., Melchiori, A.E., Siegert, F., 2018. Fuel load mapping in the Brazilian Cerrado in support of integrated fire management. *Remote Sens. Environ.* 217, 221–232.
- Furlaud, J.M., Williamson, G.J., Bowman, D.M.J.S., 2018. Simulating the effectiveness of prescribed burning at altering wildfire behaviour in Tasmania, Australia. *Int. J. Wildland Fire* 27 (1), 15.
- Gale, M.G., Cary, G.J., van Dijk, A.I.J.M., Yebra, M., 2021. Forest fire fuel through the lens of remote sensing: review of approaches, challenges and future directions in the remote sensing of biotic determinants of fire behaviour. *Remote Sens. Environ.* 255, 112282.
- García, M., Riaño, D., Chuvieco, E., Salas, J., Danson, F.M., 2011. Multispectral and LiDAR data fusion for fuel type mapping using Support Vector Machine and decision rules. *Remote Sens. Environ.* 115 (6), 1369–1379.
- García, M., Popescu, S., Riaño, D., Zhao, K., Neuenschwander, A., Agca, M., Chuvieco, E., 2012. Characterization of canopy fuels using ICESat/GLAS data. *Remote Sens. Environ.* 123, 81–89.
- Genuer, R., Poggi, J.-M., Tuleau-Malot, C., 2015. VSURF: an R package for variable selection using random forests. *R J.* 7 (2), 19–33.
- González-Ferreiro, E., Arellano-Pérez, S., Castedo-Dorado, F., Hevia, A., Vega, J.A., Vega-Nieva, D., Álvarez-González, J.G., Ruiz-González, A.D., 2017. Modelling the vertical distribution of canopy fuel load using national forest inventory and low-density airborne laser scanning data. *PLoS One* 12 (4), e0176114.
- Hanan, E.J., Kennedy, M.C., Ren, J., Johnson, M.C., Smith, A.M.S., 2022. Missing climate feedbacks in fire models: limitations and uncertainties in fuel loadings and the role of decomposition in fine fuel accumulation. *J. Adv. Model. Earth Syst.* 14 (3).
- Hardisky, M.A., Klemas, V., Smart, R.M., 1983. The influence of soil salinity, growth form, and leaf moisture on the spectral radiance of. *Photogramm. Eng. Remote. Sens.* 49 (1), 77–83.
- Heisig, J., Olson, E., Pebesma, E., 2022. Predicting wildfire fuels and hazard in a central European temperate forest using active and passive remote sensing. *Fire* 5 (1), 29.

- Hudak, A.T., Dickinson, M.B., Bright, B.C., Kremens, R.L., Loudermilk, E.L., O'Brien, J.J., Hornsby, B.S., Ottmar, R.D., 2016. Measurements relating fire radiative energy density and surface fuel consumption – RxCADRE 2011 and 2012. *Int. J. Wildland Fire* 25 (1), 25.
- Hudak, A.T., Kato, A., Bright, B.C., Loudermilk, E.L., Hawley, C., Restaino, J.C., Ottmar, R.D., Prata, G.A., Cabo, C., Prichard, S.J., Rowell, E.M., Weise, D.R., 2020. Towards spatially explicit quantification of pre- and postfire fuels and fuel consumption from traditional and point cloud measurements. *For. Sci.* 66 (4), 428–442.
- Huete, A.R., 1988. A soil-adjusted vegetation index (SAVI). *Remote Sens. Environ.* 25 (3), 295–309.
- IPCC, 2021. Summary for policymakers. In: Masson-Delmotte, V., Zhai, P., Pirani, A., Connors, A.L., Péan, C., Berger, S., Caud, N., Chen, Y., Goldfarb, L., Gomis, M.I., Huang, M., Leitzell, K., Lonnoy, E., Matthews, J.B.R., Maycock, T.K., Waterfield, T., Yelekçi, O., Yu, R., Zhou, B. (Eds.), *Climate Change 2021: The Physical Science Basis. Contribution of Working Group I to the Sixth Assessment Report of the Intergovernmental Panel on Climate Change*. Cambridge University Press.
- Jakubowski, M.K., Guo, Q., Collins, B., Stephens, S., Kelly, M., 2013. Predicting Surface Fuel Models and Fuel Metrics Using Lidar and CIR Imagery in a Dense, Mountainous Forest. *American Society for Photogrammetry and Remote Sensing*.
- Jarron, L.R., Coops, N.C., MacKenzie, W.H., Dykstra, P., 2021. Detection and quantification of coarse woody debris in natural forest stands using airborne LiDAR. *For. Sci.* 67 (5), 550–563.
- Jin, S., Chen, S.-C., 2012. Application of QuickBird imagery in fuel load estimation in the Daxinganling region, China. *Int. J. Wildland Fire* 21 (5), 583.
- Jumelle, M., Kuhn-Regnier, A., Rajaratnam, S., 2020. ALEPythoN. Python Accumulated Local Effects Package, GitHub Repository.
- ka-news, 2022. Vier Feuer im Hardtwald Karlsruhe. ka-news.
- Kauth, R.J., Thomas, G.S., 1976. The tasseled cap – a graphic description of the spectral-temporal development of agricultural crops as seen by Landsat. In: *LARS Symposia*.
- Keane, R.E., 2013. Describing wildland surface fuel loading for fire management: a review of approaches, methods and systems. *Int. J. Wildland Fire* 22 (1), 51–62.
- Keane, R.E., 2015. *Wildland Fuel Fundamentals and Applications*. Springer International Publishing, New York, NY, USA, p. 195.
- Keane, R.E., Gray, K., Bacciu, V., 2012. Spatial Variability of Wildland Fuel Characteristics in Northern Rocky Mountain Ecosystems. *Res. Pap. RMRS-RP-98*. U.S. Department of Agriculture, Forest Service, Rocky Mountain Research Station, Fort Collins, CO, 56 p. 98.
- Kim, Y., Yang, Z., Cohen, W.B., Pflugmacher, D., Lauver, C.L., Vankat, J.L., 2009. Distinguishing between live and dead standing tree biomass on the North Rim of Grand Canyon National Park, USA using small-footprint lidar data. *Remote Sens. Environ.* 113 (11), 2499–2510.
- Kislov, D.E., Korznikov, K.A., Altman, J., Vozmishcheva, A.S., Krestov, P.V., 2021. Extending deep learning approaches for forest disturbance segmentation on very high-resolution satellite images. *Remote Sens. Ecol. Conserv.* 7 (3), 355–368.
- Korpela, I., Örka, H., Maltamo, M., Tokola, T., Hyypä, J., 2010. Tree species classification using airborne LiDAR – effects of stand and tree parameters, downsizing of training set, intensity normalization, and sensor type. *Silva Fenn.* 44 (2).
- Krishna, M.P., Mohan, M., 2017. Litter decomposition in forest ecosystems: a review. *Eng. Ecol. Environ.* 2 (4), 236–249.
- Krishna Moorthy, S.M., Calders, K., Vicari, M.B., Verbeeck, H., 2020. Improved supervised learning-based approach for leaf and wood classification from LiDAR point clouds of forests. *IEEE Trans. Geosci. Remote Sens.* 58 (5), 3057–3070.
- Kruskal, W.H., Wallis, W.A., 1952. Use of ranks in one-criterion variance analysis. *J. Am. Stat. Assoc.* 47 (260), 583–621.
- Latifi, H., Hill, S., Schumann, B., Heurich, M., Dech, S., 2017. Multi-model estimation of understory shrub, herb and moss cover in temperate forest stands by laser scanner data. *Forestry* 90 (4), 496–514.
- Li, S., Wang, T., Hou, Z., Gong, Y., Feng, L., Ge, J., 2021. Harnessing terrestrial laser scanning to predict understory biomass in temperate mixed forests. *Ecol. Indic.* 121, 107011.
- Liu, H.Q., Huete, A., 1995. A feedback based modification of the NDVI to minimize canopy background and atmospheric noise. *IEEE Trans. Geosci. Remote Sens.* 33 (2), 457–465.
- Lopes Queiroz, G., McDermid, G., Linke, J., Hopkinson, C., Kariyeva, J., 2020. Estimating coarse woody debris volume using image analysis and multispectral LiDAR. *Forests* 11 (2), 141.
- Loudermilk, E.L., O'Brien, J.J., Mitchell, R.J., Cropper, W.P., Hiern, J.K., Grunwald, S., Grego, J., Fernandez-Diaz, J.C., 2012. Linking complex forest fuel structure and fire behaviour at fine scales. *Int. J. Wildland Fire* 21 (7), 882.
- Loudermilk, E.L., O'Brien, J.J., Goodrick, S.L., Linn, R.R., Skowronski, N.S., Hiern, J.K., 2022. Vegetation's influence on fire behavior goes beyond just being fuel. *Fire Ecol.* 18 (1), 1–10.
- Lutes, D.C., Keane, R.E., Caratti, J.F., 2009. A surface fuel classification for estimating fire effects. *Int. J. Wildland Fire* 18 (7), 802.
- Marino, E., Ranz, P., Tomé, J.L., Noriega, M.A., Esteban, J., Madrigal, J., 2016. Generation of high-resolution fuel model maps from discrete airborne laser scanner and Landsat-8 OLI: a low-cost and highly updated methodology for large areas. *Remote Sens. Environ.* 187, 267–280.
- McGaughey, R.J., 2022. FUSION/LDV: software for LIDAR data analysis and visualization. *Fus. Vers.* 4 (40), 217 pp.
- Mitchell, S.R., Harmon, M.E., O'Connell, K.E.B., 2009. Forest fuel reduction alters fire severity and long-term carbon storage in three Pacific Northwest ecosystems. *Ecol. Appl.* 19 (3), 643–655.
- Moghaddas, J.J., Collins, B.M., Menning, K., Moghaddas, E.E.Y., Stephens, S.L., 2010. Fuel treatment effects on modeled landscape-level fire behavior in the northern Sierra Nevada. *Can. J. For. Res.* 40 (9), 1751–1765.
- Molnar, C., 2022. *Interpretable Machine Learning. A Guide for Making Black Box Models Explainable*, 2nd ed.
- Mutlu, M., Popescu, M., Stripling, C., Spencer, T., 2008. Mapping surface fuel models using lidar and multispectral data fusion for fire behavior. *Remote Sens. Environ.* 112 (1), 274–285.
- Ottmar, R.D., 2014. Wildland fire emissions, carbon, and climate: Modeling fuel consumption. *For. Ecol. Manag.* 317, 41–50.
- Page, W.G., Alexander, M.E., Jenkins, M.J., 2013. Wildfire's resistance to control in mountain pine beetle-attacked lodgepole pine forests. *For. Chron.* 89 (06), 783–794.
- Peterson, S.H., Franklin, J., Roberts, D.A., van Wageningen, J.W., 2013. Mapping fuels in Yosemite National Park. *Can. J. For. Res.* 43 (1), 7–17.
- Plucinski, M.P., 2019. Fighting flames and forging firelines: wildfire suppression effectiveness at the fire edge. *Curr. Forest. Rep.* 5 (1), 1–19.
- Prichard, S.J., Ottmar, R.D., Anderson, G.K., 2007. *CONSUME User's Guide and Scientific Documentation*.
- R Core Team, 2022. *R: A Language and Environment for Statistical Computing*. R Foundation for Statistical Computing, Vienna, Austria.
- Reich, R.M., Lundquist, J.E., Bravo, V.A., 2004. Spatial models for estimating fuel loads in the Black Hills, South Dakota, USA. *Int. J. Wildland Fire* 13 (1), 119.
- Reinhardt, E.D. (Ed.), 1997. *First Order Fire Effects Model. FOFEM 4.0, User's Guide*. Intermountain Forest and Range Experiment Station, Forest Service, U.S. Department of Agriculture (en).
- Riaño, D., 2003. Modeling airborne laser scanning data for the spatial generation of critical forest parameters in fire behavior modeling. *Remote Sens. Environ.* 86 (2), 177–186.
- de Rigo, D., Libertá, G., Durrant, T.H., Vivancos, T.A., San-Miguel-Ayán, J., 2017. *Forest Fire Danger Extremes in Europe under Climate Change: Variability and Uncertainty*. Publications Office of the European Union, Diss., 72 pp.
- van Rossum, G., Drake, F.L., 2009. *Python 3 Reference Manual*. CreateSpace, Scotts Valley, CA.
- Rothermel, R.C., 1972. A mathematical model for predicting fire spread in wildland fuels. In: *Intermountain Forest & Range Experiment Station. Forest Service, U.S. Department of Agriculture* (en).
- Sandberg, D.V., Riccardi, C.L., Schaaf, M.D., 2007. Reformulation of Rothermel's wildland fire behaviour model for heterogeneous fuelbeds. *Can. J. For. Res.* 37 (12), 2438–2455.
- San-Miguel-Ayán, J., Durrant, T., Boca, R., Maiani, P., Libertá, G., Artés-Vivancos, T., Oom, D., Branco, A., Rigo, D., Ferrari, D., Pfeiffer, H., Grecchi, R., Nuijten, D., Onida, M., Löffler, P., 2021. *Forest Fires in Europe, Middle East and North Africa 2020*. JRC1267665, Luxembourg.
- Scott, J.H., Burgan, R.E., 2005. *Standard Fire Behavior Fuel Models. A Comprehensive Set for Use with Rothermel's Surface Fire Spread Model*. U.S. Department of Agriculture, Forest Service, Rocky Mountain Research Station (en).
- Seielstad, C.A., Queen, L.P., 2003. Using airborne laser altimetry to determine fuel models for estimating fire behavior. *J. For.* 101 (4), 10–15.
- Skowronski, N.S., Clark, K., Nelson, R., Hom, J., Patterson, M., 2007. Remotely sensed measurements of forest structure and fuel loads in the Pinelands of New Jersey. *Remote Sens. Environ.* 108 (2), 123–129.
- Stefanidou, A., Gitas, Z., Korhonen, L., Georgopoulos, N., Stavrakoudis, D., 2020. Multispectral LiDAR-based estimation of surface fuel load in a dense coniferous forest. *Remote Sens.* 12 (20), 3333.
- Strobl, C., Malley, J., Tutz, G., 2009. An introduction to recursive partitioning: rationale, application, and characteristics of classification and regression trees, bagging, and random forests. *Psychol. Methods* 14 (4), 323–348.
- Tucker, C.J., 1979. Red and photographic infrared linear combinations for monitoring vegetation. *Remote Sens. Environ.* 8 (2), 127–150.
- Tymstra, C., Bryce, R.W., Wotton, B.M., Taylor, S.W., Armitage, O.B., 2010. *Development and Structure of Prometheus: The Canadian Wildland Fire Growth Simulation Model*. Information Report NOR-X-417. Natural Resources Canada, Canadian Forest Service, Northern Forestry Centre, Edmonton, AB.
- U.S. Geological Survey, 2023. *EarthExplorer*. USGS - U.S. Geological Survey. <https://earthexplorer.usgs.gov/>. Accessed 26 May 2023 (English).
- UNEP, 2022. *Spreading like Wildfire – The Rising Threat of Extraordinary Landscape Fires*. A United Nations Environment Programme Rapid Response Assessment, Nairobi, 126 pp.
- Waldhauser, C., Hochreiter, R., Otepka, J., Pfeifer, N., Ghuffar, S., Korzeniowska, K., Wagner, G., 2014. Automated classification of airborne laser scanning point clouds. In: *Solving Computationally Expensive Engineering Problems*. Springer, Cham, pp. 269–292.
- Wallace, L., Hillman, S., Reinke, K., Hally, B., 2017. Non-destructive estimation of above-ground surface and near-surface biomass using 3D terrestrial remote sensing techniques. *Methods Ecol. Evol.* 8 (11), 1607–1616.
- Wang, D., 2020. Unsupervised semantic and instance segmentation of forest point clouds. *ISPRS J. Photogramm. Remote Sens.* 165, 86–97.
- Weinacker, H., Koch, B., Weinacker, R., 2004. *TREESVIS: A software system for simultaneous ED-real-time visualisation of DTM, DSM, laser raw data, multispectral data, simple tree and building models*. *Int. Arch. Photogramm. Remote Sens. Spat. Inf. Sci.* 36, 90–95.
- Weinmann, M., Jutzi, B., Hinz, S., Mallet, C., 2015. Semantic point cloud interpretation based on optimal neighborhoods, relevant features and efficient classifiers. *ISPRS J. Photogramm. Remote Sens.* 105, 286–304.
- Weise, D.R., Wright, C.S., 2014. Wildland fire emissions, carbon and climate: Characterizing wildland fuels. *For. Ecol. Manag.* 317, 26–40.

- Weiss, M., Baret, F., 2016. S2ToolBox Level 2 Products: LAI, FAPAR, FCOVER.
- Wing, B.M., Ritchie, M.W., Boston, K., Cohen, W.B., Gitelman, A., Olsen, M.J., 2012. Prediction of understory vegetation cover with airborne lidar in an interior ponderosa pine forest. *Remote Sens. Environ.* 124, 730–741.
- Woodall, C.W., Monleon, V.J., 2008. Sampling Protocol, Estimation, and Analysis Procedures for the Down Woody Materials Indicator of the FIA Program, Newtown Square, PA.
- You, H., Wang, T., Skidmore, A., Xing, Y., 2017. Quantifying the effects of normalisation of airborne LiDAR intensity on coniferous forest leaf area index estimations. *Remote Sens.* 9 (2), 163.
- Zeilhofer, P., Sanches, L., Vourlitis, G.L., Andrade, N.L.R., 2012. Seasonal variations in litter production and its relation with MODIS vegetation indices in a semi-deciduous forest of Mato Grosso. *Remote Sens. Lett.* 3 (1), 1–9.
- Ziegler, J.P., Hoffman, C.M., Mell, W., 2019. firebehavior: an R package for fire behavior and danger analysis. *Fire* 2 (3), 41.